Title:

Fetal imidacloprid causes ASD-like impairment of biological motion perception in neonatal chicks

Short title:

Neonicotinoid impairs neonatal vision

Authors:

Toshiya Matsushima[1,5]*, Momoko Miura[1], Nina Patzke[1,2], Noriyuki Toji[1], Kazuhiro Wada[1], Yukiko Ogura[3], Koichi J. Homma[4], Paola Sgadò[5], Giorgio Vallortigara[5]

Affiliations:

1: Department of Biology, Faculty of Science, Hokkaido University, Sapporo, Japan

2: Health and Medical University, Potsdam, Germany

3: Information Science and Technology, University of Tokyo, Tokyo, Japan

4: Department of Molecular Biology, Faculty of Pharmaceutical Sciences, Teikyo University, Tokyo, Japan

5: Center for Mind/Brain Science, University of Trento, Rovereto, Italy

*: corresponding author, e-mail: matsushimatoshiya@gmail.com

Fundings and contribution of the authors:

The present study was supported by grants funded to T.M. by the Japan Society for Promotion of Science (JSPS, Kakenhi; Grants-in-aid for Scientific Research #18K07351, #19KK0211). TM, PS and GV conceived the study. TM and MM designed the behavioral experiments and performed behavioral experiments. MM and NP performed the brain morphometry and isotropic fractionation analysis. NT, KW and KJH designed and performed molecular experiments. YO and TM made statistical analysis. TM wrote the manuscript. All authors agreed on the publication of the paper in its final form.

Declaration of the conflict of interest:

The authors declare no conflict of interest. Preprint of this paper has been uploaded at bioRxiv (https://www.biorxiv.org/content/10.1101/2022.05.19.492744v1).

Acknowledgements:

Critical comments and instructive suggestions by Dr. Brian McCabe (University of Cambridge) are highly acknowledged. Contribution of Mr. Yasutaka Sasaki (Machine Department of the Faculty of Science, Hokkaido University) must be acknowledged for production of the imprinting apparatus. We also thank Editage (www.editage.com) for English language editing.

Abstract

Several environmental chemicals are suspected as risk factors for autism spectrum disorder (ASD), including valproic acid (VPA) and pesticides acting on nicotinic acetylcholine receptor (nAChR) if exposed during pregnancy. However, their target processes in fetal neuro-development are unspecified. We report that fetal injection of VPA impaired the imprinting of an artifact object in hatchlings, while the predisposed preference to biological motion (BM) remained intact. Blockade of nAChR acted oppositely, namely, spared imprinting and impaired BM in chicks. Beside ketamine and tubocurarine, significant effects of imidacloprid (a neonicotinoid insecticide) appeared at dose ≤1ppm. Despite the distinct processes, both VPA and nAChR blockade similarly impaired imprinting of biological image composed of point-light animation. Furthermore, both impairments were rescued by post-natal bumetanide treatment, suggesting common pathology underlying the social attachment malformation. Ambient neonicotinoid could hinder adaptive socialization through impaired development of visual perception in early neonates.

Keywords:

imprinting, autism, biological motion, canalization, valproic acid, neonicotinoid, bumetanide

Introduction

Despite heterogeneous diagnostic phenotypes, autism spectrum disorder (ASD) is primarily characterized by impaired social interactions[1,2]. Visual predisposition to animate objects typically arises early in life[3-6], which is hampered in neonates/juveniles with ASD or its familial risk[7-10]. Along with genetic factors, exposure to environmental chemical agents, such as anticonvulsant (valproic acid, VPA)[11-14] and pesticides[15-18] during pregnancy is an ASD risk factor. Despite intensive efforts to develop mammalian models to assess these environmental factors[19,20], the validity is limited because these neonatal mammals (mostly rodents) do not spontaneously perceive biological motion (BM) in early life, which is found only in human neonates[3-5] and a taxonomically distant animal, domestic chicks[21].

The ability to visually perceive conspecifics, as well as identify individuals, their emotions and intention by highly reduced stimuli (such as point light animations) is referred to as the BM perception[22]. Generally, motion perception develops slowly in human neonates with early visual experiences exerting significant influences[23]. Pre-attentive processing of biologically relevant stimuli (BM and face configuration) canalizes the subsequent memorization, leading to the adaptive formation of social attachment to specific individuals[4]. Human neonates typically show an early emergence of BM preference[3,4], which most non-human animal species do not reveal. Various non-human animals discriminate BM point-light animations[24-27], but their BM perception does not spontaneously arise after birth.

In chicks, the spontaneous BM preference[21] is enhanced by imprinting of an artifact (non-BM) object[28], facilitating and canalizing the subsequent imprinting[29,30]. Along with the commonality in the early development of BM, humans[31] and chicks[32] show inversion effects, namely predisposition to up-right walking configuration. Assuming the different brain organizations between birds and humans, the functional and developmental similarities are striking. Although the neural substrates of the neonatal BM perception are largely unspecified, recent studies suggest the sub-cortical visual processing as evolutionarily conserved visual systems[33,34].

A question arises regarding this context. What prenatal processes construct the BM preference? Previous studies revealed the effects of fetal VPA application on social behaviors in chicks[35-38], but the BM preference has not been addressed. Furthermore,

if the VPA effect on the social behavioral hypoplasia was mediated by well-documented action as an inhibitor of histone deacetylation39, what other risk agents did? As VPA is a potent anti-convulsant drug, it might effectively suppress the fetal movements, hence, the BM preference. As the first step, we hypothesized that suppression of spontaneous fetal movements40,41 is responsible, where excitatory GABA actions could play a role42,43. In human adults, execution of an unfamiliar motor patterns facilitates perception of the corresponding BM animations, thus, non-visual motor execution might be involved44. According to the motor involvement, an imaging study suggested contribution of the posterior part of cerebellum in BM perception45. If this applied also to fetuses, any chemical agents that suppress spontaneous movement, including the blockade of neuro-muscular transmission, would impair the development of BM preference. We started this study by listing chemical agents that effectively suppress the fetal movement at embryonic day 14 (E14), the stage wherein VPA is reported to be effective35.

Results

Suppression of the spontaneous fetal movement by chemical agents

The fetal movement was reliably detected by placing an analog record stylus against the shell surface (experiment 1, **Figure 1A**; see supplementary for the methods and statistical analyses). Low frequency power (2~20 Hz) of the recorded signal (ballistogram46) revealed that VPA injection to the air sac acutely suppressed the movement (**Figure 1B**). Similar suppression was found by ketamine (sedative drug of a wide action spectrum including blockade of NMDAR and nAChR), mk801 (selective NMDAR blocker), and tubocurarine (nAChR blocker of a wide spectrum) (**Figure 1C**; see supplement for the chemical agents used and statistics). Among other nAChR blockers, methyllycaconitine citrate (MLA, specific to neuronal α7 subtype), and dihydro-β-erythroidine hydrobromide (DHβE, specific to muscular α4β2 subtype) were similarly effective. Fetal movement is sensitive to the blockade of cholinergic or NMDAR-mediated neurotransmission in the brain (VPA, ketamine, mk801, and MLA), and neuro-muscular junctions in the periphery (DHβE); tubocurarine can act centrally and peripherally.

BM preference and imprinting were doubly dissociated in chicks

Hatchlings of the injected eggs were tested for BM preference and imprinting (experiment 2). Chicks were individually trained by a video clip of a rotating red toy (displayed on an LCD with sound) for two hours with one hour intermission, and after 30 to 60 min, tested for BM preference (walking point-light animation over linear motion, both in white) and for imprinting memory (familiar red toy over novel yellow) (**Figure 2A**). Among the examined agents, ketamine, tubocurarine and MLA significantly reduced BM preference compared with control in a dose-dependent manner, while VPA failed (**Figure 2Ba**; see **Figure S2 and 3** for details). Despite effective suppression of the fetal movement, mk801 failed to cause any behavioral effects, and hence, VPA and ketamine should act through pathways other than NMDAR. Moreover, nAChR is responsible for the BM preference impairment because ketamine, tubocurarine and MLA were similarly effective. Notably, besides NMDAR suppression, ketamine directly blocks the nAChR-associated channels in the central nervous system and peripheral tissues47-48. However, VPA spared BM and impaired imprinting (**Figure 2Bb**), indicating that the underlying pharmacological mechanisms are doubly dissociated between these two behavioral traits, except that MLA and DHβE weakly suppressed imprinting. Suppression of fetal movements is therefore not sufficient for the BM preference impairment in hatchlings.

Distinct behavioral phenotypes appeared when imprinting score was plotted against BM score (**Figure 2Bc**). The control chicks showed a weak but significant positive correlation between the two scores (r= +0.21, p=0.0217 for n=123, Spearman's rank correlation), which was stronger in the VPA chicks (r= +0.88, p= 0.000747 for n=10) but absent in the ketamine (r= -0.042, p=0.919) and the tubocurarine chicks (r= -0.10, p=0.785). Although the cause of the individual variations was unspecified, those chicks with high BM score were resistant to VPA applied on E14. On the other hand, ketamine and tubocurarine spared the imprinting score in these chicks with low BM scores.

Blockade of nAChR transmission by imidacloprid (IMI) also impaired BM in a dose-dependent manner (**Figure 2C**). When applied to E14, IMI suppressed fetal movement at the low dose (5-50 μg/egg: ~0.1-1.0 ppm), and significantly impaired BM but spared imprinting in hatchlings. As mammalian fetus could be maternally exposed to ambient neonicotinoids, we tested the IMI effect injected into fertilized eggs before

incubation (E0). The treated hatchlings showed a significant impairment of BM at 50 μg/egg. Plotting the imprinting score against the BM (**Figure 2Cc**) revealed that the chicks with a low BM score tended to show a lower imprint score in the high-dose IMI groups (50 μg/egg), though without significant correlations (r= +0.24 and p=0.314 for E0, r= +0.18 and p= 0.623 for E14).

Bumetanide rescued both of the impairments by VPA and nAChR blockade; shared pathology at the molecular level

In concert with the excitatory nature of GABA transmission in fetus43, injection of bumetanide (blocker of a chloride cotransporter, NKCC1) on E14 also impaired the post-hatch BM preference, whereas imprinting was spared (see Supplementary material, **Figure S2C,D**), suggesting a critical importance of excitation/inhibition balance during the late phase of fetal development. When applied to P1 chicks (30 min before the start of the training session; 0.02mg/chick), on the other hand, bumetanide rescued both impairments, namely imprinting (for VPA) and BM (for ketamine and tubocurarine; **Figure 2Ba,b**). Despite distinct pathogenesis, BM and imprinting impairments could share common molecular bases associated with GABA-AR actions. Bumetanide and VU0463271 (KCC2 blocker) had no significant effects on the spontaneous movements of E14 fetuses (**Figure S1B**); suppression of the fetal movements is not necessary for the BM impairment.

Imprinting of biological motion image was impaired by both VPA and nAChR blockade; shared behavioral phenotype

BM preference canalizes the subsequent imprinting31. If chicks were trained by a non-biological artifact (rotating toy in red) on the post-hatch one day (P1), they were oriented to a biological object (walking point in yellow, Wp[yellow]) on the subsequent day (P2; experiment 3, **Figure 3**). Injection of ketamine and tubocurarine (but not VPA) on E14 suppressed BM preference on P1 (**Figure 3B**) as in experiment 2. However, the P2 training using merged point-light animations (linear motion in red and walking in yellow, Lp[red]+Wp[yellow]) resulted in the impaired formation of preference for Wp[yellow] in all groups (imprinting_1 score in **Figure 3Ca**), while preference to the artifact (red toy) remained intact except VPA (imprinting_2 score in **Da**). Multiple

regression analysis of the imprinting_1 score revealed a significant interaction of BM score and each of VPA, ketamine, and tubocurarine. VPA and nAChR blockade similarly impairs the social attachment formation to biological image via distinct neurodevelopmental processes.

Distinct effects of VPA on histone acetylation, brain size and neuronal maturation

VPA is shown to act as a potent inhibitor of histone deacetylases (HDACs)39. To see if ketamine (as nAChR blockader) could also modify HDACs, we examined histone acetylation in primary cell culture prepared from E14 embryonic telencephalon; fluorescence level was measured in randomly selected 100 cells for each treatment (experiment 4, **Figure 4A**). As expected, VPA increased the H3K27 acetylation level at a dosage comparable to the *in ovo* injection (0.12~1.2 mM of medium), whereas ketamine had no effects at 6.6 and 66 μg/mL, which was higher than the *in ovo* dose (0.2mg/50g = ca. 4 μg/mL). The VPA effect on HDACs was confirmed, whereas no comparable effects were found by ketamine.

Different brain morphology could appear in these chicks with fetal chemical treatments. Although controversial, macrocephaly (increased head/brain size) is associated with some ASD subtypes due to altered neurogenesis in the early infantile period49,50. In chicks, the whole-brain weight of hatchlings revealed that E14 injection of VPA, but not ketamine, significantly decreased the brain weight compared to control (experiment 5, **Figure 4Ba**) without changes in the body weight (**Bb**). Notably, 11 out of 53 chicks (~21%) had a distinctly small brain, whereas the rest remained in the control range. Male brains were significantly bigger, but no significant interaction occurred between sex and treatment. Isotropic fractionation revealed a significantly lower ratio of NeuN-positive cells occurred in VPA (**Figure 4Ca**) without changes in the total cell number (**Cb**). Perturbation of gene expression by VPA could lead to retardation of brain development during the late fetal stage and, hence, the delayed maturation of neurons.

In conclusion, suppression of fetal movement is not sufficient or necessary for the social attachment impairment. The present study revealed two critical neurodevelopmental processes, namely the BM predisposition and the memory

formation; the former depends on the nAChR transmission, whereas the latter is particularly fragile to VPA. Despite distinct, both processes are critical for hatchlings to form social attachments to biological objects, and share a common pathology of delayed GABA switch when impaired. Finally, imidacloprid impaired both BM and imprinting at the sublethal low dose of ≤1ppm.

Discussions

Plausible scenario of the adaptive socialization through imprinting

Since Lorenz51, imprinting has been assumed as a simple but unusual type of learning in limited precocial animals, where irreversible one-time learning occurs in a restricted short critical period after birth. This study series suggest a different figure: imprinting is composed of multiple processes and mechanisms functioning together (**Figure 5**). In the early neonatal processes, exposure to any moving object leads to the CONCPEC mechanism52 associated with the thyroid hormone (specifically, triiodo-thyronine T_3) influx, which is induced by the *primary imprinting* and, in turn, elongates the sensitive period53 and enhances innate predispositions54,55. Therefore, subsequent *secondary imprinting* is canalized to objects bearing biological features, namely, the CONLERN mechanism is activated toward adaptive social attachment. These early processes, which are homologous to that proposed for neonatal development in humans34.

Central and peripheral targets of the nAChR blockade

Nicotinic transmission is critical for neurodevelopment56,57 including the pathophysiology of ASD58,59. However, as nAChR is widespread in the brain and body60,61, several brain regions/organs must be considered. Among the possible candidates, the following regions need specific attention: (1) cholinergic neurons in the striatum and the basal forebrain projecting to wide areas in pallium (or cortex in mammals)62, (2) cholinergic neurons in nucleus isthmi parvocellularis (or pedunculo-pontine tegmental nucleus) projecting to optic tectum (superior colliculus)63, and (3) pre-ganglionic cholinergic terminals of parasympathetic nerve acting on thyroid gland64. If (1) is the case, involvement of telencephalon in the BM predisposition should be considered as delayed GABA switch may be an underlying factor in the brain

areas along with IMM, arco and tectum. If (2), retarded visual attention due to the underdeveloped tecto-isthmo-tectal network must be considered. If (3), hypothyroidism during gestation or early neonatal period could be the target as reported in human neonates65,66 and chicks53. The responsible regions' specification will enable us to design appropriate amendments for each phenotype.

Neonicotinoids could cause ASD via neonatal vision

Environmental risk of neonicotinoids was initially related to the population decline of insectivorous birds67 and the delayed migration by impaired foraging behavior68. Recently, the association between ambient neonicotinoids and ASD in humans has been identified in several extensive epidemiological studies69-71. Fetal/neonatal exposure of acetamiprid neonicotinoid caused abnormal development of socio-sexual behavior in mice72. Despite the low level of acute toxicity, low affinity for vertebrate nAChR, and rapid metabolism73, neonicotinoids are known for a high persistence level. As shown in this study, identical effective dosage appeared in the E0 and E14 groups of IMI treatment (**Figure 2C**). IMI suppressed BM preference nearly completely at 1ppm (1mg/kg egg weight), which was significantly lower than the lethal dose (LD_{50} <44 mg/kg/day in red-legged partridges) and even lower than the dose (8.8mg/kg/day) that reduced immune response of the offspring74. Legislation on the control of residual neonicotinoids and other pesticidal chemicals in feed, meat, and eggs should consider the risk of increase in the ASD cases by nicotinic blockers.

Advantages and limitations of chicks for screening of ASD risk agents

This study suggests that the domestic chick is a valid animal model75,76 for studying ASD, even though birds are taxonomically distant from humans. (1) Chick has construct validity because there are common causes and processes, such as VPA, blockade of nAChR, and involvement of GABA transmission. (2) Chick uniquely has face validity because BM preference and learned social attachment formation are assayed. (3) Chick has predictive validity because bumetanide rescued the impairments by VPA and nAChR blockade. We must also consider the recent development of a rich repertoire of behavioral paradigms available in domestic chicks77-79, ranging from numerical comprehension, arithmetic, and the link of the social rank to cognitive

capability. ASD is characterized by the impaired social interactions and other symptoms such as delayed speech, learning disability, repetitive stereotyped behaviors, and altered (reduced or sensitized) sensory perception, which we may address using chicks as the model, including a longitudinal life-long survey of these treated chicks.

Although inferior in the homological validity76, the chick model has several technical advantages over conventional mammalian models. (1) Maternal complication is disregarded, whereas gestational effects are inevitably subjected to the maternal metabolism in mammals. (2) The time course and effective dose of agents are precisely determined. (3) The short incubation period facilitates speedy screening, as it takes only a week from the injection of chemicals to E14 eggs until the hatchling are tested on P1. (4) Simple imprinting paradigm allows testing of predisposed preference and learning ability. Humans are often exposed to several ASD risk factors simultaneously. The chick model is suitable for examining interactions of these agents in a strictly controlled manner by monitoring heterogeneous aspects of the disabilities.

Figure legends

Figure 1. Suppression of the spontaneous fetal movement by chemical agents. **(A, B)** Ballistography recording (experiment 1) and blockade by sodium valproate (VPA). Record stylus placed against the eggshell surface detected the miniature vibration caused by spontaneous fetal movement. **(C)** The dose was experimentally searched for each agent so that fetal movement was similarly suppressed on embryonic day 14 (E14), wherein the treatment gave rise to normal hatch rate and successful training of the hatchlings. Asterisks indicate the significant difference from the control by multiple regression analysis; *, $p<0.05$, **, $p<0.01$, ***, $p<0.001$. Number in parenthesis indicates the sample size.

Figure 2. BM preference and imprinting were doubly dissociated in chicks. Effects of the fetal injection of chemical agents on the biological motion (BM) preference and imprinting memory were examined in the hatchlings. **(A)** Training and test procedures (experiment 2). Chicks were trained by an artifact object (rotating red toy) and tested by binary choices for BM (walking motion vs linear motion) and imprinting (red toy vs yellow); stay time difference (sec) was used for the scores. **(B)**

BM **(a)** and imprinting score **(b)** of the treated hatchlings were plotted (**c**). Horizontal lines indicate the critical levels of the control data determined by bootstrap computation; average (blue), 95% (brown) and 99% (red) confidence levels. Distinct spectrums were found between VPA and other agents. **(C)** Imidacloprid (IMI) also suppressed BM **(a)** if injected on E0 or E14. Although not significant, imprinting was slightly suppressed by IMI 50μg in both injection days **(b)**.

Figure 3. Imprinting of biological motion image was impaired by both VPA and nAChR blockade.

The two-step imprinting paradigm revealed common hypoplasia by E14 injection of VPA and nAChR blockade (experiment 3). **(A)** Behavioral procedure. After the post-hatch 1-day (P1) training using an artifact (rotating red toy) and BM test, chicks received the second day (P2) training, wherein two images of point light animations were presented with yellow in walking (Wp[yellow]) and red in linear rigid motion (Lp[red]). **(B)** BM scores confirmed the experiment 2. **(Ca,b)** Both VPA and ketamine chicks showed the impaired formation of preference to Wp[yellow]. Notably, the tubocurarine chicks showed similar plots to the ketamine. (**Da,b**) VPA chicks showed the impaired imprinting to artifact red toy as in experiment 2.

Figure 4. Distinct effects of VPA on brain size, matured neuron ratio, histone acetylation, and expression of chloride co-transporter genes.

(A,B) VPA but not ketamine/tubocurarine reduced the brain weight **(Aa)**, and the ratio of NeuN positive cells measured by isotropic fractionation **(Bb)**; body weight **(Ab)** and total cell number **(Ba)** were not affected. Male brains were significantly heavier, but no interaction was found between the sex and the agents. No significant effects of sex were detected on the cell number and the NeuN ratio. **(C)** VPA but not ketamine enhanced the acetylation level of histone H3K27 in primary cell culture made from E14 telencephalon. **(D)** Expression of chloride cotransporters (ratio of NKCC1/KCC2 for *slc12a2*/*slc12a5*; **Cb**) was compared in hatchlings after VPA **(Da)** and tubocurarine **(Db)** injection on E14. Marginally significant interaction (p=0.067) was found in the tectum of VPA chicks.

Figure 5. Plausible scenario of the adaptive socialization through imprinting.

Reference list

1. Wing L, Gould J. (1979). Severe impairments of social interaction and associated abnormalities in children: epidemiology and classification. *Journal of Autism and Developmental Disorders* 9: 11-29 (https://doi.org/10.1007/BF01531288)
2. American Psychiatric Association. Diagnostic and Statistical Manual of Mental Disorders. 5th ed. Washington: *American Psychiatric Association*; 2013.
3. Simion F, Regolin L, Bulf H. (2008). A predisposition for biological motion in the newborn baby. *Proceedings of the National Academy of Sciences* 105: 809-813 (https://doi.org/10.1073/pnas.0707021105)
4. Bardi L, Regolin L, Simion F. (2011). Biological motion preference in humans at birth: role of dynamic and configural properties. *Developmental Science* 14: 353-359 (https://doi.org/10.1111/j.1467-7687.2010.00985.x)
5. Sifre R, Olson L, Gillespie S, Klin A, Jones W, Shultz S. (2018). A longitudinal investigation of preferential attention to biological motion in 2- and 24-month-old infants. *Scientific Reports* 8: 2527 (https://doi.org/10.1038/s41598-018-20808-0)
6. Di Giorgio E, Lunghi M, Vallortigara G, Simion F. (2021). Newborns' sensitivity to speed changes as a building block for animacy perception. *Scientific Reports* 11: 542 (https://doi.org/10.1038/s41598-020-79451-3)
7. Rutherford MD, Pennington BF, Rogers SJ. (2006). The perception of animacy in young children with autism. Journal of Autism and Developmental Disorders 36: 983–992 (https://doi.org/10.1007/s10803-006-0136-8)
8. Klin A, Lin DJ, Gorrindo P, Ramsay G, Jones W. (2009). Two-year-olds with autism orient to non-social contingencies rather than biological motion. *Nature* 459: 257–261 (https://doi.org/10.1038/nature07868)
9. Di Gioggio E, Frasnelli E, Rosa-Salva O, Scattoni ML, Puopolo M, Tosoni D, NIDA-Network, Simion F, Vallortigara G. Difference in visual social predispositions between newborns at low- and high-risk for autism. (2016). *Scientific Reports* 6: 26395 (https://doi.org/10.1038/srep26395)
10. Wang Y, Wang L, Xu Q, Liu D, Chen L, Troje NF, He S, Jiang Y. (2018) Heritable aspects of biological motion perception and its covariation with autistic traits. *Proceedings of the National Academy of Sciences* 115: 1937-1942 (https://doi.org/10.1073/pnas.1714655115).
11. Moore SJ, Turnpenny P, Quinn A, Glover S, Lloyd DJ, Montgomery T, Dean JCS. (2000). A clinical study of 57 children with fetal anticonvulsive syndromes. *Journal of Medical Genetics* 37: 489-497 (https://doi.org/10.1136/jmg.37.7.489)
12. Rasalam AD, Hailey H, Williams JHG, Moore SJ, Turnpenny PD, Lloyd DJ, Bean JCS. (2005). Characteristics of fetal anticonvulsant syndrome associated autistic disorder. *Developmental Medicine & Clinical Neurology* 47: 551-555 (https://doi.org/10.1017/S0012162205001076)
13. Bromley RL, Mawer GE, Briggs M, Cheyne C, Clayton-Smith J et al. (2013). The prevalence of neurodevelopmental disorders in children prenatally exposed to antiepileptic drugs. *Journal of Neurology, Neurosurgery & Psychiatry* 84: 637-643 (https://doi.org/10.1136/jnnp-2012-304270)
14. Christensen J, Grønborg TK, Sørensen MJ, Schendel D, Parner ET, Pedersen LH Vestergaard M. (2013) Prenatal valproate exposure and risk of autism spectrum

disorders and childhood autism. *Journal of the American Medical Association* 309: 1696-1703 (https://doi.org/10.1001/jama.2013.2270)
15. Keil AP, Daniels JL, Hertz-Picciotto I. (2014) Autism spectrum disorder, flea and tick medication, and adjustments for exposure misclassification: the CHARGE (Childhood Autism Risks from Genetics and Envinronment) case-control study. *Environmental Health* 13:3 (https://doi.org/10.1186/1476-069X-13-3)
16. GunierRB, Bradman A, Harley KG, Kogut K, Eskenazi B. (2017). Prenatal residential proximity to agricultural pesticide use and IQ in 7-year-old children. *Environmental Health Perspectives* (https://doi.org/10.1289/EHP504)
17. von Ehrenstein OS, Ling C, Cui X, Cockburn M, Park AS, Yu F, Wu J, Ritz B. (2019). Prenatal and infant exposure to ambient pesticides and autism spectrum disorder in children: population based case-control study. 364:l962 (https://doi.org/10.1136/bmj.l962) 364:l962
18. Ongono JS, Béranger R, Baghdadli A, Mortamais M. (2020) Pesticides used in Europe and autism spectrum disorder risk: can novel exposure hypotheses be formulated beyond organophosphates, organochlorines, organochlorines, pyrethroids and carbamates? – A systematic review. Environmental Research 187: 209646 (https://doi.org/10.1016/j.envres.2020.109646)
19. Nicolini C, Fahnestock M. (2018). The valproic acid-induced rodent model of autism. *Experimental Neurology* 299: 217-227 (https://doi.org/10.1016/j.expneurol.2017.04.017)
20. Chaliha D, Albrecht M, Vaccarezza M, Takechi R, Lam V, Al-Salami H, Mamo J. (2020) A systematic review of the valproic acid-induced rodent model of autism. *Developmental Neuroscience* 42:12–48 (https://doi.org/10.1159/000509109)
21. Vallortigara G, Regolin L, Marconato F. (2005). Visually inexperienced chicks exhibit spontaneous preference for biological motion patterns. *Plos Biology* 3: e208 (https://doi.org/10.1371/journal.pbio.0030208)
22. Johansson G. (1973). Visual perception of biological motion and a model for its analysis. *Perception & Psychophysics* 14: 201-211 (https://doi.org/10.3758/BF03212378)
23. Hadad B, Schwartz S, Mauer D, Lewis TL. (2015). Motion perception: a review of developmental changes and the role of early visual experience. *Frontiers in Integrative Neuroscience* 9: 49 (https://doi.org/10.3389/fnint.2015.00049)
24. Dittrich WH, Lea SEG, Barrett J, Gurr PR. (1998). Categorization of natural movements by pigeons: visual concept discrimination and biological motion. *Journal of Experimental Analysis of Behavior* 70:281–299 (https://doi.org/10.1901/jeab.1998.70-281)
25. Parron C, Deruelle C, Fagot J. (2007). Processing of biological motion point-light displays by baboons (Papio papio). *Journal of Experimental Psychology: Animal Behavior Processes* 33:381–391 (https://doi.org/10.1037/0097-7403.33.4.381)
26. MacKinnon LM, Troje NF, Dringenberg HC. (2010). Do rats (*Rattus norvegicus*) perceive biological motion? *Experimental Brain Research* 205:571–576 (https://doi.org/10.1007/s00221-010-2378-0)
27. Nunes AR, Carreira L, Anbalagan S, Blechman J, Levkowitz G, Oliveira RF. (2020). Perceptual mechanisms of social affiliation in zebrafish. *Scientific Reports* 10: 3642 (https://doi.org/10.1038/s41598-020-60154-8)
28. Miura M, Matsushima T. (2012). Preference for biological motion in domestic

chicks: sex-dependent effect of early visual experience. *Animal Cognition* 15: 871-879. (https://doi.org/10.1007/s10071-012-0514-x)
29. Miura M, Matsushima T. (2016). Biological motion facilitates imprinting. *Animal Behaviour* 116: 171-180 (https://doi.org/10.1016/j.anbehav.2016.03.025)
30. Miura M, Nishi D, Matsushima T. (2020). Combined predisposed preferences for colour and biological motion make robust development of social attachment through imprinting. *Animal Cognition* 23: 169-188 (doi https://doi.org/10.1007/s10071-019-01327-5)
31. Troje NF, Westhoff C. (2006). The inversion effect in biological motion perception: evidence for a “life detector”? *Current Biology* 16: 821-824 (https://doi.org/10.1016/j.cub.2006.03.022)
32. Vallortigara G, Regolin L. (2006). Gravity bias in the interpretation of biological motion by inexperienced chicks. *Current Biology* 16: R279-R280 (https://doi.org/10.1016/j.cub.2006.03.052)
33. Chang DHF, Ban H, Ikegaya Y, Fujita I, Troje NF. (2018). Cortical and subcortical responses to biological motion. *Neuroimage* 174: 87-96 ()
34. Hirai M, Senju A. (2020). The two-process theory of biological motion processing. *Neuroscience and Biobehavioral Reviews* 111: 114-124. (https://doi.org/10.1016/j.neubiorev.2020.01.010)
35. Nishigori H, Kagami K, Takahashi A, Tezuka Y, Sanbe A, Nishigori H. (2013). Impaired social behavior in chicks exposed to sodium valproate during the last week of embryogenesis. *Psychopharmacology* 227: 393-402 (https://doi.org/10.1007/s00213-013-2979-y)
36. Lorenzi E, Pross A, Rosa-Salva O, Versace E, Sgadò P, Vallortigara G. (2019). Embryonic exposure to valproic acid affects social predispositions for dynamic cues of animale motion in newly-hatched chicks. *Frontiers in Physiology* 10: 501 (https://doi.org/10.3389/fphys.2019.00501)
37. Sgadò P, Rosa-Salva O, Versace E, Vallortigara G. (2019). Embryonic exposure to valproic acid impairs social predispositions of newly-hatched chicks. *Scientific Reports* 8:5919 (https://doi.org/10.1038/s41598-018-24202-8)
38. Adiletta A, Pedrana S, Rosa0Salva O, Sgadò P. (2021). Spontaneous visual preference for face0like stimuli is impaired in newly-hatched domestic chicks exposed to valproic acid during embryogenesis. *Frontiers in Behavioral Neuroscience* 15: 733140 (https://doi.org/10.3389/fnbeh.2021.733140)
39. Phiel CJ, Zhang F, Huang EY, Guenther MG, Lazar MA, Klein PS. (2001). Histone deacetylase is a direct target of valproic acid, a potent anticonvulsant, mood stabilizer, and teratogen. *Journal of Biological Chemistry* 28: 36734–36741 (https://doi.org/10.1074/jbc.M101287200)
40. Bekoff A, Stein PSG, Hamburger V. (1975). Coordinated motor output in the hindlimb of the 7-day chick embryo. *Proceedings of the National Academy of Sciences of the United States of America* 72: 1245-1248 (https://doi.org/10.1073/pnas.72.4.1245)
41. Blankenship AG, Feller MB. (2010). Mechanisms underlying spontaneous patterned activity in developing neural circuits. *Nature Reviews Neuroscience* 11: 18-29 (https://doi.org/10.1038/nrn2759)
42. Ben-Ari Y. (2002). Excitatory actions of GABA during development: the nature of the nurture. *Nature Reviews Neuroscience* 3: 728-739

(https://doi.org/10.1038/nrn920)
43. Represa A, Ben-Ari Y. (2005). Tropic actions of GABA on neuronal development. *Trends in Neuroscience* 28: 278-283 (https://doi.org/10.1016/j.tins.2005.03.010)
44. Casile A, Giese MA. (2006). Nonvisual motor training influences biological motion perception. *Current Biology* 16: 69-74 (https://doi.org/10.1016/j.cub.2005.10.071)
45. Jack A, Keifer CM, Pelphrey KA. (2017) Cerebellar contributions to biological motion perception in autism and typical development. *Human Brain Mapping* 38:1914-1932 (https://doi.org/10.1002/hbm.23493)
46. Suzuki Y, Musashi H, Tazawa H. (1989). Noninvasive heart rate monitoring system for avian embryos based on the ballistocardiogram. *Medical and Biological Engineering & Computing* 27: 399-404
47. Scheller M, Bufler J, Hertle I, Schneck H, Franke C, Kochs E. (1996). Ketamine blocks currents through mammalian nicotinic acetylcholine receptor channels by interaction with both the open and the closed state. *Anesthesia & Analgesia* 83: 830-836 (https://doi.org/10.1097/00000539-199610000-00031)
48. McMillan R, Muthukumaraswamy SD. (2020). The neurophysiology of ketamine: an integrative review. *Reviews in the Neurosciences* 31: 457-503. (https://doi.org/10.1515/revneuro-2019-0090)
49. Courchesne E, Carper R, Akshoomoff N. (2003). Evidence of brain overgrowth in the first year of life in autism. *Journal of American Medical Association*, 290: 337-344 (https://doi.org/10.1001/jama.290.3.337)
50. Klein S, Sharifi-Hannauer P, Martinez-Agosto JA. (2013). Macrocephaly as a clinical indicator of genetic subtypes in autism. *Autism Research* 6: 51-56 (https://doi.org/10.1002/aur.1266)
51. Lorenz K. (1937). The companion in the bird's world. *Auk* 54: 245–273 (https://doi.org/10.2307/40780 77)
52. Morton J, Johnson MH. (1991). CONSPEC and CONLERN: a two-process theory of infant face recognition. *Psychological Review* 98: 164-181 (https://doi.org/10.1037/0033-295X.98.2.164)
53. Yamaguchi S, Aoki N, Kitajima T, Iikubo E, Katagiri S, Matsushima T, Homma KJ. (2012). Thyroid hormone determines the start of the sensitive period of imprinting and primes later learning. *Nature Communications* 3: 1081 (https://doi.org/10.1038/ncomms2088)
54. Miura M, Aoki N, Yamaguchi S, Homma K-J, Matsushima T. (2018). Thyroid hormone sensitizes the imprinting-associated induction of biological motion preference in domestic chicks. *Frontiers in Physiology (Avian Physiology)* 9:1740 (https://doi.org/10.3389/fphys.2018.01740)
55. Takemura Y, Yamaguchi S, Aoki N, Miura M, Homma KJ, Matsushima T. (2018). Gene expression of Dio2 (thyroid hormone converting enzyme) in telencephalon is linked with predisposed biological motion preference in domestic chicks. *Behavioural Brain Research* 349: 25-30 (https://doi.org/10.1016/j.bbr.2018.04.039)
56. Liu Z, Neff RA, Berg DK. (2006). Sequential interplay of nicotinic and GABAergic signaling guides neuronal development. *Science* 314: 1610-1613 (https://doi.org/10.1126/science.1134246)
57. Dwyer JB, McQuown SC, Leslie FM. (2009). The dynamic effects of nicotine on the developing brain. *Pharmacology & Therapeutics* 122: 125-139 (https://doi.org/10.1016/j.pharmthera.2009.02.003)

58. Karvat G, Kimchi T. (2014). Acetylcholine elevation relieves cognitive rigidity and social deficiency in a mouse model of autism. *Neuropsychophamacology* 39: 831-840. (https://doi.org/10.1038/npp.2013.274)
59. Marotta R, Risoleo MC, Messina G, Parisi L, Carotenuto M, Vetri L, Roccella M. (2020). The neurochemistry of autism. *Brain Sciences* 10: 163 (https://doi.org/10.3390/brainsci10030163)
60. Millar NS, Gotti C. (2009). Diversity of vertebrate nicotinic acetylcholine receptors. *Neuropharmacology* 56: 237-246 (https://doi.org/10.1016/j.neuropharm.2008.07.041)
61. Fisher SK, Wonnacott S. (2012). Acetylcholine. In: Basic Neurochemistry, 8th edition. (eds: Brady ST et al.) Elsevier Masson pp.258-282. (https://doi.org/10.1016/B978-0-12-374947-5.00013-4)
62. Ahmed NY, Knowles R, Dehorter N. (2019). New insights into cholinergic neuron diversity. *Frontiers in Molecular Neuroscience* 12: 204 (https://doi.org/10.3389/fnmol.2019.00204)
63. Knudsen EI. (2011). Control from below: the role of a midbrain network in spatial attention. *European Journal of Neuroscience* 33: 1961–1972 (https://doi.org/10.1111/j.1460-9568.2011.07696.x)
64. IImura K, Suzuki H, Hotta H. (2019). Thyroxin and calcitonin secretion into thyroid venous blood is regulated by pharyngeal mechanical stimulation in anesthetized rats. *Journal of Physiological Sciences* 69: 749-756 (https://doi.org/10.1007/s12576-019-00691-8)
65. Román GC, Ghassabian A, Bongers-Schokking JJ, Jaddoe VWV, Hofman A, de Rijke YB, Verhult FC, Tiemeir H. (2013). Association of gestational maternal hypothyroxinemia and increased autism risk. *Annals of Neurology* 74: 733-742 (https://doi.org/10.1002/ana.23976)
66. Getahun D, Jacobson SJ, Fassett MJ, Wing DA, Xiang AH, Chiu VY, Peltier MR. (2018). Association between maternal hypothyroidism and autism spectrum disorders in children. Pediatric Research 83: 580–588 (https://doi.org/10.1038/pr.2017.308)
67. Hallmann CA, Foppen RPB, van Turnhaut CAM, de Kroon H, Jongejans E. (2014). Declines in insectivorous birds are associated with high neonicotinoid concentration. *Nature* 511: 341-343 (https://doi.org/10.1038/nature13531)
68. Eng ML, Stutchbury BJM, Morrissey CA. (2019). A neonicotinoid insecticide reduces fueling and delays migration in songbirds. *Science* 365: 1177-1180 (https://doi.org/10.1126/science.aaw9419)
69. Gunier RB, Bradman A, Harley KG, Kogut K, Eskenazi B. (2017). Prenatal residential proximity to agricultural pesticides use and IQ in 7-year-old children. *Environmental Health Perspectives* 125: 5 (https://doi.org/10.1289/EHP504)
70. von Ehrenstein OS, Ling C, Cui X, Cockburn M, Park AS, Yu F, Wu J, Ritz B. (2019). Prenatal and infant exposure to ambient pesticides and autism spectrum disorder in children: population based case-control study. *the BMJ* 364: 1962 (http://dx.doi.org/10.1136/bmj.l962)
71. Ongono JS, Béranger R, Baghdadli A, Mortamais M. (2020). Pesticides used in Europe and autism spectrum disorder risk: can novel exposure hypotheses be formulated beyond organophosphates, organochlorines, pyrethroids and carbamates? – A systematic review. *Environmental Research* 187: 109646

(https://doi.org/10.1016/j.envres.2020.109646)
72. Sano K, Isobe T, Yang J, Win-Shwe T, Yoshikane M, Nakayama SF, Kawashima T, Suzuki G, Hashimoto S, Nohara K, Tohyama C, Maekawa F. (2016). In utero and lactational exposure to acetamiprid induces abnormalities in socio-sexual and anxiety-related behaviors of male mice. *Frontiers in Neuroscience* 10: 228 (https://doi.org/10.3389/fnins.2016.00228)
73. Bean TG, Gross MS, Karouna-Renier NK, Henry PFP, Schultz SL, Hladik ML, Kuivila KM, Rattner BA. (2019). Toxicokinetics of imidacloprid-coated wheat seeds in Japanese quail (*Coturnix japonica*) and an evaluation of hazard. *Environmental Science & Technology* 53: 3888-3897 (https://doi.org/10.1021/acs.est.8b07062)
74. Lopez-Antia A, Ortiz-Santaliestra ME, Mougeot F, Mateo R. (2015). Imidacloprid-treated seed ingestion has lethal effect on adult partridges and reduces both breeding investment and offspring immunity. *Environmental Research* 136: 97-107 (http://doi.org/10.1016/j.envres.2014.10.023)
75. Willner P. (1984). The validity of animal models of depression. *Psychopharmacology* 83: 1-16 (https://doi.org/10.1007/BF00427414)
76. Belzung C, Lemoine M. (2011). Criteria of validity for animal models of psychiatric disorders: focus on anxiety disorders and depression. *Biology of Mood & Anxiety Disorders* 1: 9 (https://doi.org/10.1186/2045-5380-1-9)
77. Rugani R, Fontanari L, Simoni E, Regolin L, Vallortigara G. (2009). Arithmetic in newborn chicks. *Proceedings of the Royal Society B* 276: 2451-2460 (https://doi.org/10.1098/rspb.2009.0044)
78. Rugani R. (2017). Towards numerical cognition's origin: insights from day-old domestic chicks. *Philosophical Transactions B* 373: 20160509 (https://doi.org/10.1098/rstb.2016.0509)
79. Daisley JN, Vallortigara G, Regolin L. (2021). Low-rank *Gallus gallus domesticus* chicks are better at transitive inference reasoning. *Communications Biology* 4: 1344 (https://doi.org/10.1038/s42003-021-02855-y)

Reference cited in the supplementary material

- Herculano-Houzel S, Lent R. (2005). Isotropic fractionator: a simple, rapid method for the quantification of total cell and neuron numbers in the brain. *Journal of Neuroscience* 25: 2518-2521 (doi: 10.1523/JNEUROSCI.4526-04.2005)

Supplementary materials: Methods and Statistical Analyses

1. Methods

1.1.Animals and compliance with ethical standard

Experiments were conducted under the guidelines and approval of the Committee on Animal Experiments of Hokkaido University (approval number 20-0141). The guidelines are based on the national regulations for animal welfare in Japan (Law for Humane Treatment and Management of Animals, after partial amendment No. 68, 2005). Number of subjects used are indicated below in the statistical analyses for each experiment.

Domestic white Leghorn chicks (*Gallus gallus domesticus*, an egg-laying strain of Leghorn called "Julia") were used. Fertilized eggs were purchased from a local hatchery (Iwamura Co., Niigata/Hokkaido Japan) every 2 weeks, and the batch was numbered. Eggs were incubated in the laboratory by using type P-008B incubators (Showa Furanki Co., Saitama Japan) with its temperature controlled at 37.7°C and the humidity at ca. 80%. The inside of the incubator was kept in complete darkness until hatch. Chicks were individually hatched in small boxes separated by black plastic walls, so that they could interact acoustically but not visually. To avoid post-hatch visual experiences, hatchlings were individually housed in boxes placed in another incubator of the same type, kept in darkness until the experiment. Chicks were sexed after the experiment. Generally, fertilized eggs weighed 59.8 ± 3.1 g (mean ± s.d., n=170) and ca. 2 g lighter at embryonic 14 days (E14) whereas the shells weighed 8.0 ± 0.1 g (n=16), so that the wet weight is assumed to be around 50 g. In this series of experiments, as the egg weight did not considerably vary, the amount of injected chemical per egg was fixed and not adjusted for each egg.

1.2. Ballistographic recording of embryonic movements (experiment 1)

Mechanical vibration caused by spontaneous fetal movements were recorded following the ballistocardiogram method developed by Suzuki et al. (1989; reference #47). By a micromanipulator, an analog record stylus cartridge (type AT VM95E, Audio Technica Co., Tokyo Japan) was gently pushed against the shell of egg placed on a thin rubber membrane, which was stretched on a glass jar (**Figure 1A**). The jar and the manipulator were firmly settled on a heavy iron plate and housed in a constant temperature incubator at 37.7°C and high humidity. The recorded monoaural signal was amplified by a hand-made low input-impedance amplifier (made of FET operational amplifier, TL084), band-pass filtered (cut-off frequency: 10~100Hz, magnification: x1,000), and stored at 1,000 point/sec sampling rate by Spike2 (ver.7, the interface CED-1401 micro3, Cambridge Electric Design Co., Cambridge UK). Frequency spectrum of 2-20 Hz range was monitored, and the converted power was stored at every 1 sec (**Figure 1B**). Using R as platform (see below), the power value was averaged at every 1 min, and the temporal profiles were constructed for pre-injection 30 min and post-injection 90 min for each egg.

Superimposed traces of the ballistographic recordings obtained from 9 sets of fetuses are shown in **Figure S1A**. Dose dependency of the suppressive effects of injected chemicals are shown in **Figure S1B**.

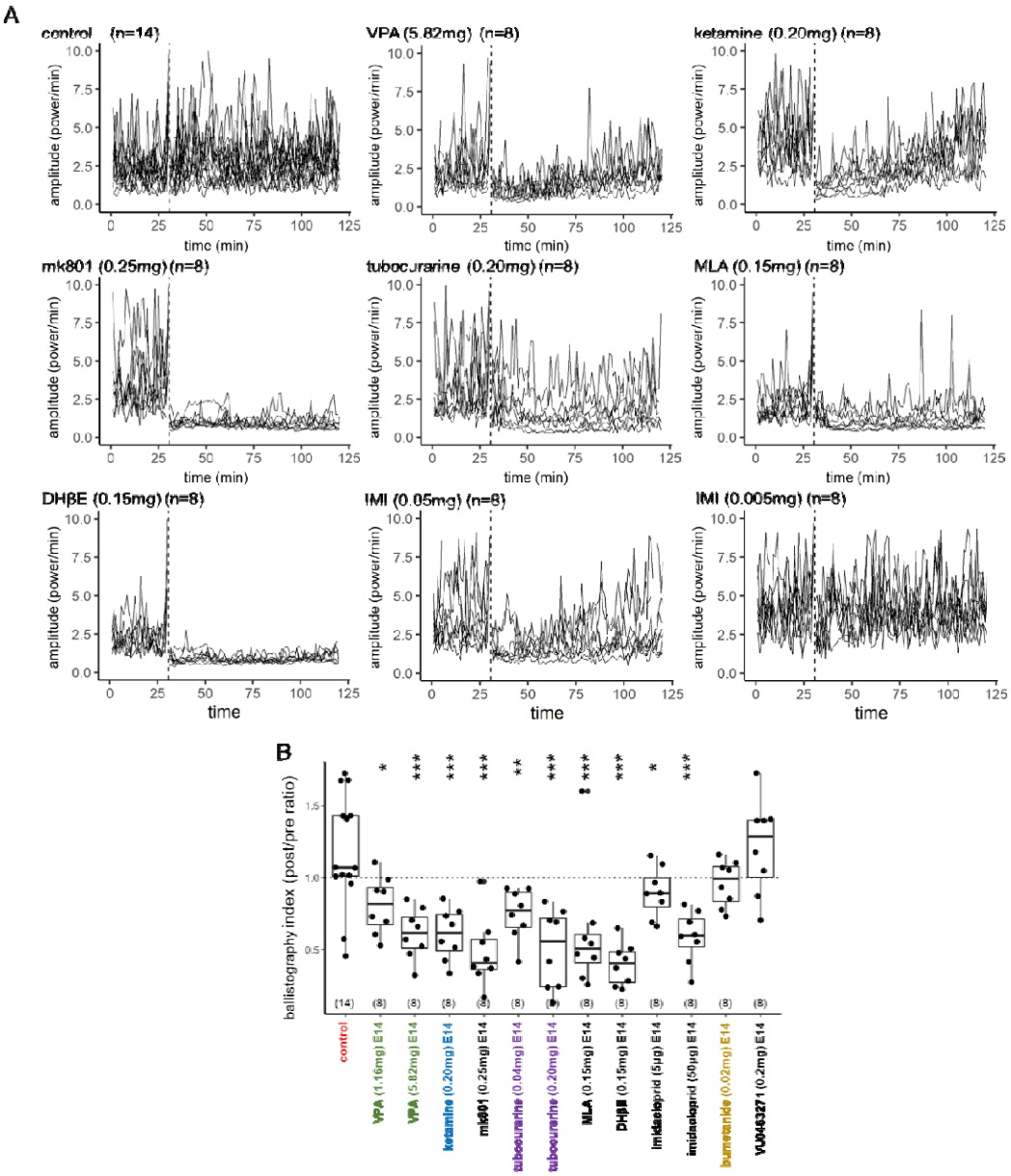

Figure S1

1.3.Apparatus and procedures of imprinting and tests (experiment 2 and 3)

An I-shaped maze (10 cm wide, 70 cm long) was equipped with a 50-cm-long treadmill consisting of a rubber belt at the center and an LCD monitor at each end (**Figure 2Aa**) and placed in a dark room at 27~28°C. See our previous reports for details (Miura et al., 2018, 2020; Takemura et al. 2018; reference #31,54,55). Two training sessions (1 hour each) were given at 1 hour interval. An infrared sensor and a transparent Plexiglass partition were placed at a point 10 cm from one monitor, and the other monitor was occluded by an opaque partition. A loudspeaker behind the LCD

monitor emitted mechanical sound synchronized with the toy movement on the screen. When chicks approached the monitor and hit the sensor, the rubber belt of the treadmill moved for a short period of 1.0 s, drawing the chick backward by about 30 cm at a time with the shortest intervals set at 0.1~2 sec. The apparatus was controlled by Arduino®. The treadmill motions were digitally counted, and the number of approaches was recorded for each chick. We monitored the chick behavior via a video camera set at the ceiling.

After 30 min to 1 hour pause period in a dark chamber kept at ~30°C, the trained chicks were tested in binary choice using the same apparatus without treadmill motions. In the BM test, one monitor displayed a linear point-light animation and the other monitor a walking one, both composed of white lights. In the subsequent imprinting test, one monitor displayed red toy (familiar object) and another yellow (novel object), both unaccompanied by the mechanical sound used in training. We consider that the subject chose one side when the whole body was located close (<30 cm) to the monitor (delineated by dashed line). Five-min tests were repeated twice after swapping the side, and the initial side was also counterbalanced among individuals. Tests were video-recorded. Intervals between test trials were set at 90-120sec. The difference in stay times gave the choice score in sec thus ranging in -600 to +600 sec.

In experiment 2, chicks were trained and tested on post-hatch 1 day (P1, at 12~36 hours after hatch) by the procedure shown in **Figure 2Ab**. In experiment 3, chicks were similarly trained and tested for the BM preference on P1, then re-trained by merged Lp(red) and Wp(yellow) on P2 (**Figure 3A**); the chicks were simultaneously exposed to two point-light animations, one walking in yellow Wp(yellow) and another linear in red Lp(red). Our recent study (Miura et al. 2020; reference #31) revealed that chicks exposed to the merged animations showed significantly higher preference to Wp[yellow] over Lp[red], if the BM preference of the chicks had been induced by the training using the red toy on P1.

1.4.Video clips and point-light animations for training and tests

Two video clips of a rotating toy and 3 point-light animations were prepared as in our previous reports (Miura and Matsushima 2016, Miura et al. 2018, 2020; reference #30,31,54); see below for the list. Video clips were displayed on black background at a speed of 30 frames/s. We made editing by Adobe Premiere (Elements 7) and the color was set either to red (R: 255, G: 0, B: 0) or yellow (R: 255, G: 255, B: 0). These stimuli were displayed on the LCD monitors (size 10.4”, 800 × 600 pixels, Logitec LCM-T102AS, Japan; flash rate: 56–75 Hz, brightness: 230 cd/m2, pitch size: 0.264 × 0.264 mm) using free viewer software (A-player, version 6.0) on PC. The width of the presentation was set at 10.5 cm on the monitor, the surface of which was placed at 2.0 cm away from the terminal window of the maze.

Moving-toy(red).wmv	P1 training and imprinting test (experiment 2,4)
Moving-toy(yellow).wmv	imprinting test (experiment 2,4)
Wp(white).wmv	BM test (experiment 2,4)
Lp(white).wmv	BM test (experiment 2,4)
Wp(yellow)-Lp(red).wmv	P2 training (experiment 4)
Wp(yellow).wmv	imprinting_1 (biological) test (experiment 4)
Lp(red).wmv	imprinting_1 (biological) test (experiment 4)

1.5.Chemical agents

Eggs (embryonic 14 days, E14, if not stated otherwise) received single injection of 200μL solution to the air chamber through one of two holes on the round edge of the shell; another hole served as air vent for smooth injection. The holes were sealed by mending tape. For each agent, the highest dosage was determined which (1) did not reduce the rate of hatching and (2) significantly suppressed the spontaneous fetal motions, then 1/5 diluted solution was tested. Control eggs received injection of the same amount of vehicle, distilled water.

Name, code and company of the chemical agents

chemical name	code number	company
VPA (sodium valproate)	cas no.1069-66-5	FUJIFILM Wako Pure Chemical Co.
ketamine (hydrochloride)	ATC code N01AX03	Daiichi-Sankyo Propharma Co.
mk801 ((+)-mk801 maleate)	cas no. 77086-22-7	FUJIFILM Wako Pure Chemical Co.
tubocurarine (D-tubocurarine chloride pentahydrate)	cas no. 41354-45-4	FUJIFILM Wako Pure Chemical Co.
MLA (methyllycaconitine citrate)	cas no. 112825-05-5	abcam
DHβE (dihydro-β-erythroidine hydrobromide)	cas no. 29734-68-7	TOCRIS Biocscience
imidacloprid (standard)	cas no. 105827-78-9	FUJIFILM Wako Pure Chemical Co.
bumetanide	cas no. 28395-03-1	TOCRIS Bio-techne
VU0463271	cas no. 1391737-01-1	TOCRIS Neuroscience

Amount of agents injected / egg ~ 50g

chemical agent	molecular weight	μmole
VPA 5.82mg	166.19	35.0
ketamine 0.20mg	274.19	0.729
mk801 0.25mg	337.37	0.741
tubocurarine 0.20mg	771.72	0.259
MLA 0.15mg	874.92	0.171
DHβE 0.15mg	356.26	0.421
imidacloprid 0.05mg	255.66	0.196
bumetanide 0.02mg	364.42	0.0549
VU0463271 0.2mg	387	0.517

1.6.Histone acetylation assay in cultured brain cells (experiment 4)

Embryos (E7 and E14) were aseptically harvested from eggs and brain tissues were separated. Brain tissues were finely minced with scissors in sterile phosphate-buffered saline (PBS) and dissociated by pipetting with micropipette tips. Dissociated brain tissues were suspended in a brain culture medium composed of DMEM/F12 (048-29785, FUJIFILM Wako Pure Chemical Co., Tokyo, Japan), 10% foetal bovine serum (S-FBS-NL-015, Serana Europe GmbH, Brandenburg, Germany), 1x Antibiotic-Antimycotic (15240-096, Life Technologies Co., CA, USA), and maintained on coverslip glasses coated with collagen type I-C (631-00771, FUJIFILM Wako Pure Chemical Co., Tokyo, Japan) for 4 days at 37°C in 5% CO_2 condition.

The cultured brain tissues were incubated with ketamine (66 or 6.6 μg/mL), VPA (1.2 mM or 0.12 mM) or vehicle PBS in a brain culture medium without FBS for 2 hours at 37°C in 5% CO_2. After incubation, cultured brain tissues were fixed with 4% paraformaldehyde in PBS for 5 mins, blocked with a blocking solution (4% normal goat serum (S-1000, VECTOR laboratories Inc., CA, USA), 1% blocking reagent (1096176, Roche Ltd., Basel, Swiss) and 0.5% Tween20 in PBS) for 30 mins, and then incubated with 1:3000 diluted Anti-acetyl Histone H3 (Lys27), mouse monoclonal antibody (MA309A, TaKaRa Bio Inc., Shiga, Japan) in the blocking solution for 16 hours at 4□ in a humidity chamber. Following the first antibody incubation, tissues were incubated with 1:2000 diluted Goat anti-Mouse IgG, Alexa Fluor 555 antibody (A21422, ThermoFisher Scientific, MA, USA) in the blocking solution for 2 hours at room temperature in a humidity chamber. Stained tissues were mounted in Mounting Medium with DAPI (H-1200, VECTOR Laboratories Inc.) and imaged using a BZ-X810 microscope (Keyence Co., Osaka, Japan). In each duplicated experimental group, three fields of view were taken per coverslip, and the acetylation level of H3K27 in the nuclei of 100 randomly selected cells from six fields of view was measured as fluorescence intensity using Image J.

1.7.Brain weight and isotropic fractionation measurement of brain cells (experiment 5 and 6)

The P1 chicks were transcardially perfused by 4% paraformaldehyde in 0.1M phosphate buffer under a deep anesthesia by i.m. injection of 0.8mL ketamine-xylazine cocktail; a 1:1 mixture of 10mg/mL ketamine hydrochloride (Daiichi-Sankyo Propharma Co.) and 2mg/mL xylazine (Sigma-Aldrich Co.).

The whole brain (cut at the caudal end of medulla oblongata) was dissected and post-fixed in the fixative for overnight, stored for 2~4 days in phosphate-buffered saline (PBS) at 4°C and weighed. The telencephalon was isolate at the rostral level of diencephalon and manually chopped in small pieces by scalpel. The tissue was weighed and homogenized in a detergent solution (40mM sodium citrate and 1% Triton X-100) using a 7mL glass Tenbroeck tissue homogenizer. The homogenate and several washes of the homogenizer were transferred to a 50ml falcon tube using a glass pipette. To visualize cell nuclei DAPI (4,6-diamidino-2-phenylindoledihydrochloride, Invitrogen, Carlsbad, Calif., USA) was added to the suspension from a stock solution at 20 mg/L (dilution 1:20 to 1:50) and the final volume of the suspension was recorded. To estimate the total amount of cells in the suspension, the nuclear density was quantified in a

Neubauer chamber by a fluorescent microscope (BX-50, Olympus Co., Tokyo, Japan) according to the protocol developed by Herculano-Houzel and Lent (2005).

To estimate the number of matured neuron, aliquot (500 μL) of the nuclear suspension washed with PB (0.1M) and incubated overnight in the dark at 4°C with Cy3-labeled rabbit polyclonal neuronal nuclear antigen antibody (1:150 dilution; NeuN, RRID:AB_11204707). The percentage of neuronal nuceli was determined by counting at least 500 DAPI-stained nuclei and establishing the fraction that was also NeuN positive, according to the protocol developed by Herculano-Houzel and Lent (2005). Briefly, the total number of neurons in each sample was determined by multiplying the total number of cells in the structure by the NeuN-positive fraction obtained. The total number of non-neuronal cells was determined by subtracting the total number of neurons from the total number of cells. Densities of neurons and non-neurons (cell/mg) were determined by dividing the number of neurons or non-neurons by the mass (mg) of the structure.

2. Statistical analyses

Statistical computations were performed on RStudio version 3.6.3 (2020-02-29). For single and multiple regression analyses, linear models were constructed using the function *lm()* with the control group as the reference set; one model was calculated for each set of experimental groups. Multiple regression including variables such as *sex*, *batch* and *run* (locomotor counts during training) appeared not to improve the statistical judgements; we therefore adopted single regression by *drug* (and dose) in most cases.

In experiment 6, where gene expression profiles were examined, IMM and E14 served the reference for the brain region and the age, respectively. Significance is coded as 0 < *** < 0.001 < ** < 0.01 < * <0.05, and ns means p-value ≥ 0.05.

2.1. Experiment 1

2.1.1. Ballistography index explained by drug (Figure 1C)

fit_exp_1_ballistography_selected <- lm(ratio ~ label, data = dataset_exp_1_ballistography_fig)
summary(fit_exp_1_ballistography_selected)
Coefficients:

label (drug)	estimate	std. error	t-value	Pr(>|t|)	signif. code
(intercept)	+1.18063	0.07899	14.947	< 2e-16	***
VPA 5.82mg	-0.56805	0.13099	-4.337	6.23e-05	***
ketamine 0.20mg	-0.57210	0.13099	-4.368	5.60e-05	***
mk801 0.25mg	-0.69986	0.13099	-5.343	1.80e-06	***
tubocurarine 0.20mg	-0.67630	0.13099	-5.163	3.46e-06	***
MLA 0.15mg	-0.56939	0.13099	-4.347	6.01e-05	***
DHβE 0.15mg	-0.78066	0.13099	-5.960	1.87e-07	***

residual standard error = 0.2956 (Df = 55)
multiple r-squared = 0.5006, adjusted r-squared = 0.4461
F-statistic = 9.188 (Df = 6, 55), p-value = 5.765e-07

2.2 Experiment 2, VPA, ketamine and tubocurarine (Figure 2B)

2.2.1. BM score explained by drug (Figure 2Ba)

fit_exp2_bm_selected <- lm (bm ~ label, data = dataset_exp_2_bm_imprint_fig)
summary (fit_exp2_bm_selected)
Coefficients:

drug	estimate	std. error	t-value	Pr(>|t|)	signif. code
(intercept)	136.309	16.187	8.415	6.86e-15	***
VPA 5.82mg	26.091	59.075	0.442	0.65920	ns
VPA 5.82mg +bumetanide	-53.709	59.075	-0.909	0.36434	ns
ketamine 0.20mg	-146.809	59.075	-2.485	0.01375	*
ketamine 0.20mg +bumetanide	-92.854	56.537	-1.642	0.10206	ns
mk801 0.25mg	-9.509	59.075	-0.161	0.87228	ns
tubocurarine 0.20mg	-162.509	59.075	-2.751	0.00648	**
tubocurarine 0.20mg +bumetanide	-71.109	59.075	-1.204	0.23010	ns
MLA 0.15mg	-153.509	59.075	-2.599	0.01005	*
DHβE 0.15mg	-50.309	59.075	-0.852	0.39543	ns

residual standard error = 179.7 (Df=204)
multiple r-squared = 0.09335, adjusted r-squared = 0.05335
F-statistic = 2.334 (Df = 9, 204), p-value = 0.01597

2.2.2. imprinting score explained by drug (Figure 2Bb)

fit_exp2_imprint_selected <- lm (imprint ~ label, data = dataset_exp_2_bm_imprint_fig)
summary (fit_exp2_imprint_selected)
Coefficients:

drug	estimate	std. error	t-value	Pr(>|t|)	signif. code
(intercept)	419.52	19.80	21.183	< 2e-16	***
VPA 5.82mg	-316.22	72.22	-4.378	1.91e-05	***
VPA 5.82mg +bumetanide	84.68	72.22	1.172	0.2424	ns
ketamine 0.20mg	-118.62	72.22	-1.642	0.1020	ns
ketamine 0.20mg +bumetanide	-26.07	69.12	-0.377	0.7065	ns
mk801 0.25mg	3.88	72.22	0.054	0.9572	ns
tubocurarine 0.20mg	47.08	72.22	0.652	0.5152	ns
tubocurarine 0.20mg +bumetanide	-5.42	72.22	-0.075	0.9402	ns
MLA 0.15mg	-160.32	72.22	-2.220	0.0275	*
DHβE 0.15mg	-151.02	72.22	-2.091	0.0378	*

residual standard error = 219.6 (DF = 204)
multiple r-squared = 0.1348, adjusted r-squared = 0.09664
F-statistic = 3.532 (DF = 9, 204), p-value = 0.0004322

2.3. Experiment 2, imidacloprid (Figure 2C)

2.3.1. BM score explained by drug (Figure 2Ca)

fit_exp_3_bm <- lm (bm ~ label, data = dataset_exp_2_bm_imprint_ctrl_imi)
summary (fit_exp_3_bm)
Coefficients:

drug	estimate	std. error	t-value	Pr(>|t|)	signif. code
(intercept)	117.66	21.05	5.589	1.42e-07	***
E0 IMI 0.005mg	-28.25	47.90	-0.590	0.5564	ns
E0 IMI 0.05mg	-109.98	45.82	-2.400	0.0179	*
E14 IMI 0.005mg	-114.16	59.92	-1.905	0.0591	ns
E14 IMI 0.05mg	-137.06	59.92	-2.288	0.0239	*

residual standard error = 177.4 (DF = 122)
multiple r-squared = 0.08534, adjusted r-squared = 0.05535
F-statistic =2.846 (DF = 4, 122), p-value = 0.02689

2.3.2. imprinting score explained by drug (Figure 2Cb)

fit_exp_3_imprint <- lm (imprint ~ label, data = dataset_exp_2_bm_imprint_ctrl_imi)
summary (fit_exp_3_imprint)
Coefficients:

drug	estimate	std. error	t-value	Pr(>|t|)	signif. code
(intercept)	417.03	28.98	14.390	<2e-16	***
E0 IMI (0.005mg)	+20.74	65.94	0.314	0.754	ns
E0 IMI (0.05mg)	-99.03	63.08	-1.570	0.119	ns
E14 IMI (0.005mg)	-60.13	82.48	-0.729	0.467	ns
E14 IMI (0.05mg)	-101.13	82.48	-1.226	0.223	ns

residual standard error = 244.2 (DF = 122)
multiple r-squared = 0.03378, adjusted r-squared = 0.0021
F-statistic = 1.066 (DF = 4, 122), p-value = 0.3762

2.4. Bootstrapping analysis of Experiment 2

We made post-hoc bootstrapping analysis of the control data (123 chicks) to obtain the distribution (probability density) of the mean of samples composed of n=10 chicks. For each of BM and imprinting scores, 10 chicks were randomly sampled 10,000 times from the control data. For each sample from 10 chicks, difference between the sample average (n=10) and the average of the unsampled chicks (n=113) were calculated, thus yielding a set of 10,000 values. Distribution of the difference value was represented as

probability density curves shown below (**Figure S2**), and the critical points where the area below the curve occupied 95% and 99% were obtained by using *quantile()*.

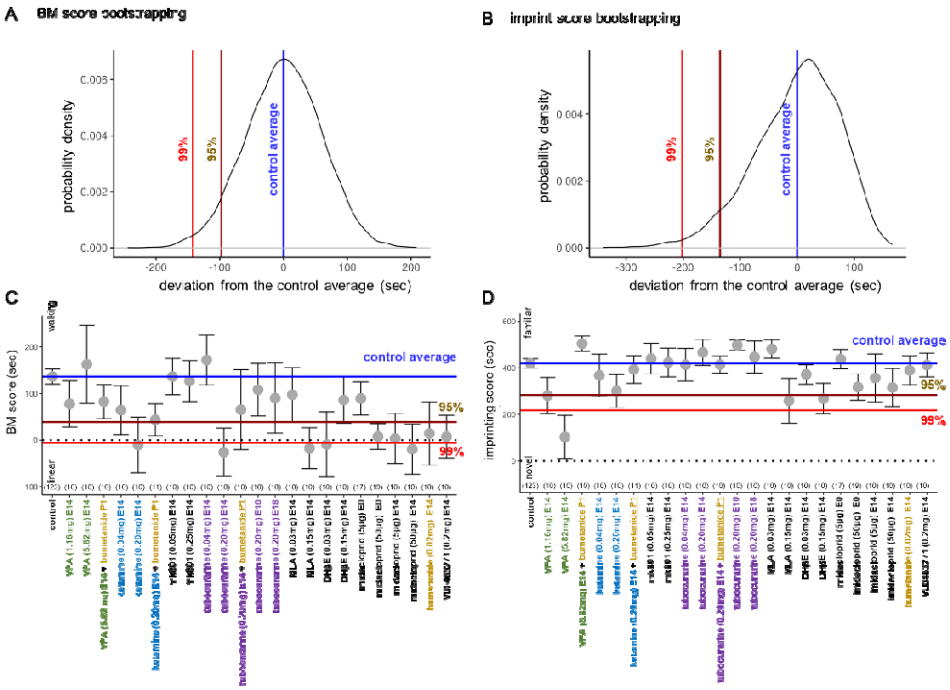

Figure S2

2.5. Experiment 3 (Figure 3)

2.5.1. BM score explained by drug (Figure 3B)

fit_exp4_bm_drug <- lm(bm ~ drug, data = dataset_exp_4_double_imprint)
summary (fit_exp4_bm_drug)
Coefficients:

drug	estimate	std. error	t-value	Pr(>|t|)	signif. code
control	145.80	52.24	2.791	0.00781	**
VPA 5.82mg	-18.22	78.37	-0.232	0.81729	ns
ketamine 0.20mg	-172.30	82.61	-2.086	0.04296	*
tubocurarine 0.20mg	-235.00	82.61	-2.845	0.00678	**

residual standard error = 202.3 (DF = 43)
multiple r-squared = 0.2076, adjusted r-squared = 0.1523
F-statistic =3.755 (DF = 3, 43), p-value = 0.01758

2.5.2. imprinting_1 (biological) score explained by drug (Figure 3Ca)

fit_exp4_imprint_1 <- lm(imprint_1 ~ drug, data = dataset_exp_4_double_imprint)
summary (fit_exp4_imprint_1)
Coefficients:

drug	estimate	std. error	t-value	Pr(>|t|)	signif. code
control	37.13	59.77	0.621	0.5377	ns

VPA 5.82mg	-213.05	89.66	-2.376	0.0220	*
ketamine 0.20mg	-201.53	94.51	-2.132	0.0387	*
tubocurarine 0.20mg	-60.33	94.51	-0.638	0.5266	ns

residual standard error = 231.5 (DF = 43)
multiple r-squared = 0.1533, adjusted r-squared = 0.09428
F-statistic = 2.596 (DF = 3, 43), p-value = 0.06465

2.5.3. imprinting_1 (biological) score explained by drug and BM score (Figure 3Cb)

*fit_exp4_imprint_1_bm <- lm(imprint_1 ~ drug * bm, data = dataset_exp_4_double_imprint)*
summary (fit_exp4_imprint_1_bm)
Coefficients:

drug/BM	estimate	std. error	t-value	Pr(>|t|)	signif. code
(intercept)	-128.6864	72.0850	-1.785	0.082007	ns
VPA 5.82mg	-1.7390	99.4170	-0.017	0.986134	ns
ketamine 0.20mg	-36.8073	98.1233	-0.375	0.709609	ns
tubocurarine 0.20mg	104.6133	103.3479	1.012	0.317660	ns
BM	1.1373	0.3286	3.462	0.001317	**
VPA*BM	-1.4939	0.4161	-3.591	0.000911	***
ketamine*BM	-1.1786	0.4706	-2.505	0.016545	*
tubocurarine*BM	-1.1471	0.5003	-2.293	0.027323	*

residual standard error = 208.6 (DF = 39)
multiple r-squared = 0.3764, adjusted r-squared = 0.2645
F-statistic = 3.363 (DF = 7, 39), p-value = 0.00668

2.5.4. imprinting_2 (artifact) score explained by drug (Figure 3Da)

fit_exp4_imprint_2 <- lm(imprint_2 ~ drug, data = dataset_exp_4_double_imprint)
summary (fit_exp4_imprint_2)
Coefficients:

drug	estimate	std. error	t-value	Pr(>|t|)	signif. code
control	487.13	68.66	7.095	9.38e-09	***
VPA 5.82mg	-277.38	102.99	-2.693	0.0100	*
ketamine 0.20mg	-194.93	108.56	-1.796	0.0796	ns
tubocurarine 0.20mg	-91.23	108.56	-0.840	0.4053	ns

residual standard error = 265.9 (DF = 43)
multiple r-squared = 0.1582, adjusted r-squared = 0.09942
F-statistic = 2.693 (DF = 3, 43), p-value = 0.0579

2.5.5. imprinting_2 (artifact) score explained by drug and BM (Figure 3Db)

*fit_exp4_imprint_2_bm <- lm(imprint_2 ~ drug*bm, data = dataset_exp_4_double_imprint)*
summary (fit_exp4_imprint_2_bm)

Coefficients:

drug/BM	estimate	std. error	t-value	Pr(>|t|)	signif. code
(intercept)	470.3160	93.4620	5.032	1.13e-05	***
VPA 5.82mg	-320.8333	128.8993	-2.489	0.0172	*
ketamine 0.20mg	-179.5913	127.2220	-1.412	0.1660	ns
tubocurarine 0.20mg	-103.0923	133.9960	-0.769	0.4463	ns
BM	0.1153	0.4260	0.271	0.7880	ns
VPA*BM	0.3570	0.5394	0.662	0.5120	ns
ketamine*BM	-0.1710	0.6101	-0.280	0.7807	ns
tubocurarine*BM	-0.4368	0.6486	-0.673	0.5046	ns

residual standard error = 270.5 (DF = 39)
multiple r-squared = 0.21, adjusted r-squared = 0.06819
F-statistic = 1.481 (DF = 7, 39), p-value = 0.2026

2.6. Experiment 4 (Figure 4A)

H3K27ac fluorescence explained by drug

fit_exp_5_h3k27ac <- lm(flu ~ drug, data = dataset_exp_5_h3k27ac)
summary(fit_exp_5_h3k27ac)

Coefficients:

drug	estimate	std. error	t-value	Pr(>|t|)	signif. code
(intercept)	+7.4293	0.3156	23.537	<2e-16	***
VPA 0.12mM	+0.5917	0.4464	1.326	0.186	ns
VPA 1.2mM	+11.9921	0.4464	26.865	<2e-16	***
ketamine 6.6 μg/mL	□ 0.4920	0.4464	□ 1.102	0.271	ns
ketamine 66 μg/mL	+0.0230	0.4464	0.052	0.959	ns

residual standard error = 3.156 (DF = 495)
multiple r-squared = 0.7, adjusted r-squared = 0.6975
F-statistic = 288.7 (DF=4, 495), p-value: < 2.2e-16

2.7.Experiment 5 and 6 (Figure 4B,C)

2.7.1. brain weight (Figure 4Ba)

*fit_exp_6_abs_w_brain <- lm (w_brain ~ sex * drug, data = dataset_exp_6_brain_weight)*
summary (fit_exp_6_abs_w_brain)

Coefficients:

drug/sex	estimate	std. error	t-value	Pr(>|t|)	signif. code
(intercept)	1.00174	0.01520	65.887	< 2e-16	***
sex	0.03101	0.02135	1.453	0.148404	ns
VPA 5.82mg	-0.08410	0.02426	-3.467	0.000683	***
ketamine 0.20mg	-0.04889	0.02891	-1.691	0.092845	ns
tubocurarine	-0.03094	0.04246	-0.729	0.467397	ns

0.20mg					
sex* VPA	0.02942	0.03266	0.901	0.369059	ns
sex* ketamine	0.01340	0.03939	0.340	0.734245	ns
sex* tubocurarine	0.02419	0.06000	0.403	0.687336	ns

residual standard error = 0.08865 (DF = 153)
multiple r-squared = 0.1514, adjusted r-squared = 0.1126
F-statistic= 3.901 (Df = 7, 15), p-value = 0.0006117

2.7.2. body weight (Figure 4Bb)

*fit_exp_6_abs_w_body <- lm (w_body ~ sex * drug, data = dataset_exp_6_brain_weight)*
summary (fit_exp_6_abs_w_body)
Coefficients:

drug/sex	estimate	std. error	t-value	Pr(>|t|)	signif. code
(intercept)	39.65882	0.54955	72.166	<2e-16	***
sex	0.17832	0.87678	0.231	0.818	ns
VPA 5.82mg	-1.3451	0.02426	-1.534	0.127	ns
ketamine 0.20mg	-0.06652	0.02891	-0.064	0.949	ns
tubocurarine 0.20mg	1.10118	1.53481	0.717	0.474	ns
sex* VPA	0.85643	1.18040	0.726	0.469	ns
sex* ketamine	-1.36438	1.42373	-0.958	0.339	ns
sex* tubocurarine	-1.91832	2.16856	-0.885	0.378	ns

Residual standard error = 3.204 (DF = 153)
multiple r-squared = 0.03717, adjusted r-squared = -0.006877
F-statistic= 0.8439 (Df = 7, 153), p-value = 0.5527

2.7.3. NeuN-positive cell ratio (Figure 4Ca)

*fit_exp_6_neuron_glia_ratio <- lm(neuron_ratio ~ sex * drug, data = dataset_exp_6_neuron_glia)*
summary (fit_exp_6_neuron_glia_ratio)
Coefficients:

drug/sex	estimate	std. error	t-value	Pr(>|t|)	signif. code
(intercept)	0.522874	0.019104	27.370	<2e-16	***
sex	-0.073903	0.027017	0.632	0.5316	ns
VPA 5.82mg	-0.073903	0.027017	-2.735	0.0101	*
ketamine 0.20mg	0.008096	0.027017	0.300	0.7664	ns
tubocurarine 0.20mg	-0.001942	0.027017	-0.072	0.9431	ns
sex* VPA	0.025310	0.038208	0.662	0.5124	ns
sex* ketamine	-0.055518	0.038208	-1.453	0.1559	ns
sex* tubocurarine	-0.017455	0.038208	-0.457	0.6509	ns

residual standard error=0.04272 (DF = 32)
multiple r-squared = 0.3429, adjusted r-squared = 0.1991
F-statistic: 2.385 (Df=7, 32), p-value = 0.04411

2.7.4. total cell number (Figure 4Cb):

*fit_exp_6_cell_count <- lm(cell_number ~ sex * drug, data = dataset_exp_6_neuron_glia)*
summary (fit_exp_6_cell_count)
Coefficients:

drug/sex	estimate	std. error	t-value	Pr(>|t|)	signif. code
(intercept)	32.806	3.128	10.488	6.97e-12	***
sex	3.626	4.424	0.820	0.418	ns
VPA 5.82mg	-0.599	4.424	-0.135	0.893	ns
ketamine 0.20mg	-1.412	4.424	-0.319	0.752	ns
tubocurarine 0.20mg	2.088	4.424	0.472	0.640	ns
sex* VPA	-2.719	6.256	-0.435	0.667	ns
sex* ketamine	-2.004	6.256	-0.320	0.751	ns
sex* tubocurarine	-5.436	6.256	-0.869	0.391	ns

residual standard error=6.994 (DF = 32)
multiple r-squared = 0.05307, adjusted r-squared = -0.1541
F-statistic= 0.2562 (Df = 7, 32), p-value = 0.9663

figure_1

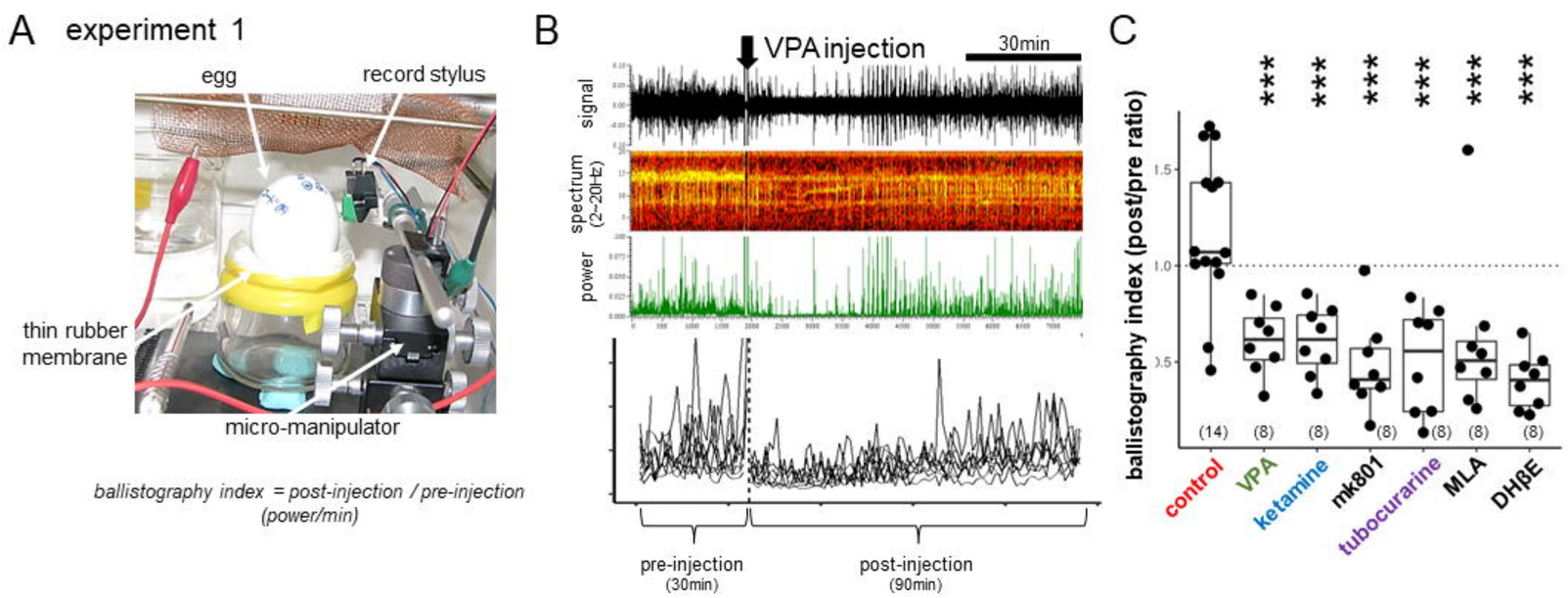
A
experiment 1
egg
record stylus
thin rubber membrane
micro-manipulator
ballistography index = post-injection / pre-injection (power/min)
B
VPA injection
30min
signal
spectrum (2~20Hz)
power
pre-injection (30min)
post-injection (90min)
C
ballistography index (post/pre ratio)
1.5
1.0
0.5
***
(14)
(8)
control
VPA
ketamine
mk801
tubocurarine
MLA
DHβE

figure_2

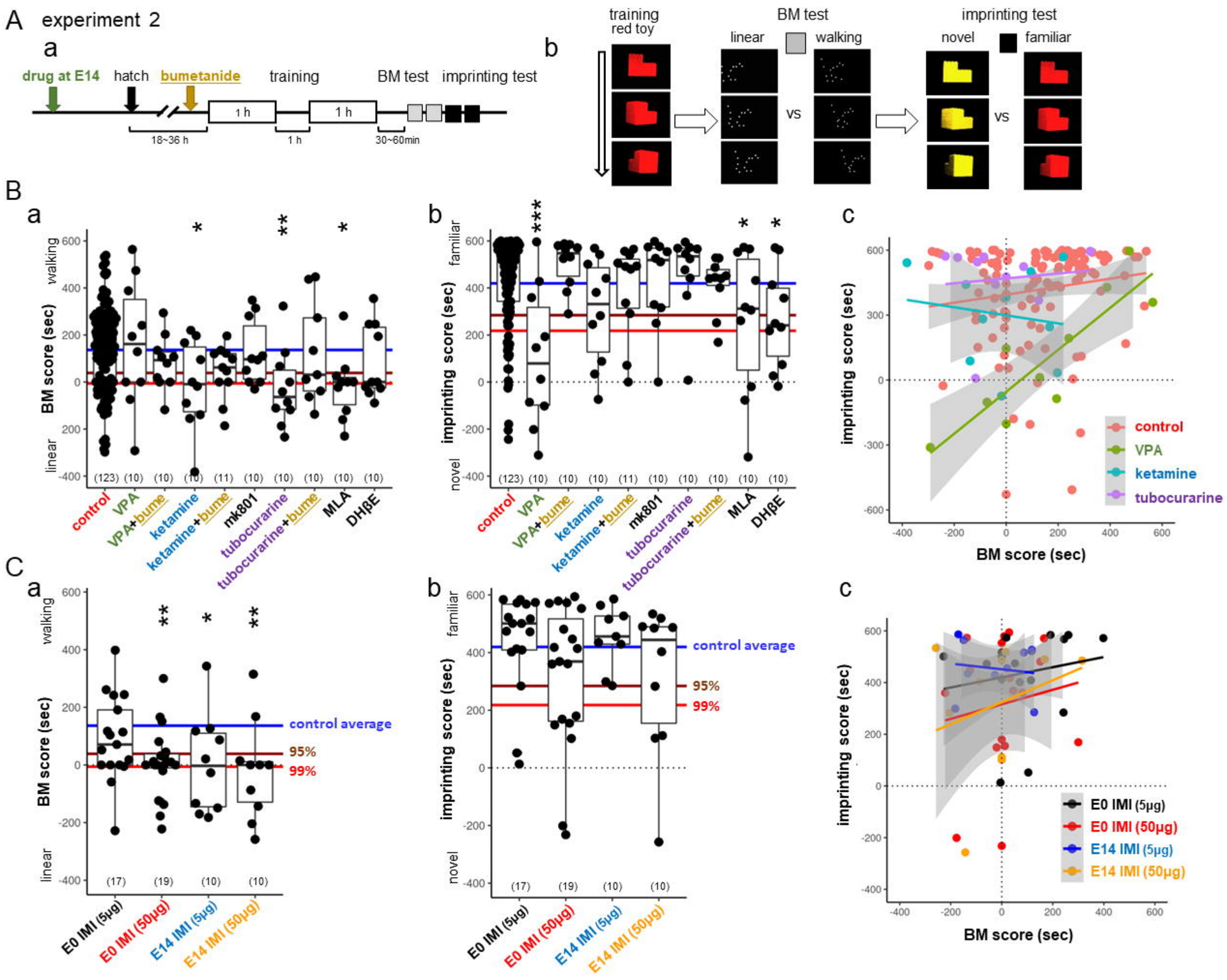
A experiment 2
a
drug at E14
hatch
bumetanide
training
BM test
imprinting test
1 h
1 h
18~36 h
1 h
30~60min
b
training
red toy
BM test
linear
walking
vs
imprinting test
novel
familiar
vs
B
a
BM score (sec)
walking
linear
control
VPA
VPA+bume
ketamine
ketamine+bume
mk801
tubocurarine
tubocurarine+bume
MLA
DHβE
b
imprinting score (sec)
familiar
novel
c
imprinting score (sec)
BM score (sec)
control
VPA
ketamine
tubocurarine
C
a
BM score (sec)
walking
linear
control average
95%
99%
E0 IMI (5μg)
E0 IMI (50μg)
E14 IMI (5μg)
E14 IMI (50μg)
b
imprinting score (sec)
familiar
novel
control average
95%
99%
c
imprinting score (sec)
BM score (sec)
E0 IMI (5μg)
E0 IMI (50μg)
E14 IMI (5μg)
E14 IMI (50μg)

figure_3

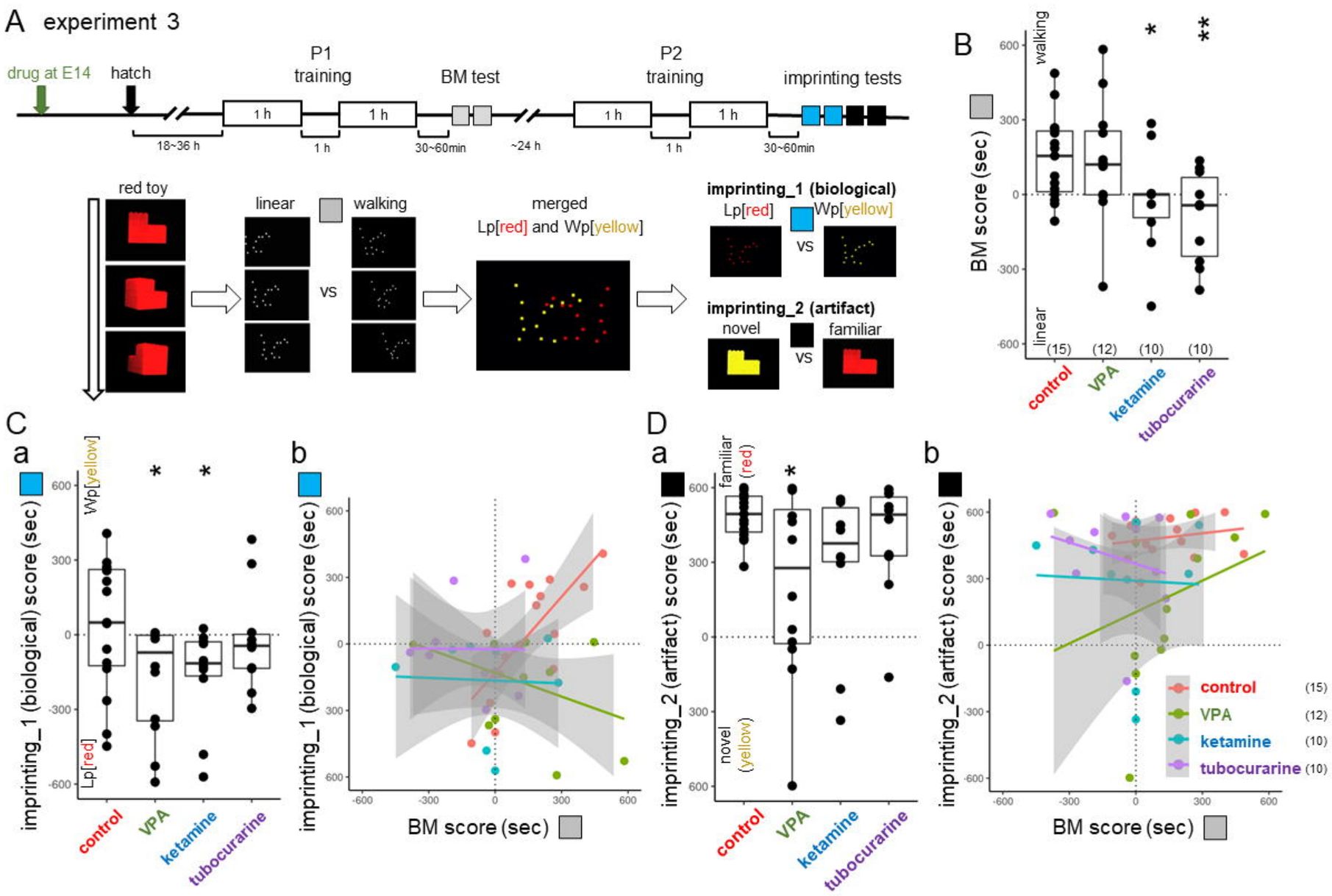
A experiment 3
drug at E14
hatch
P1 training
BM test
P2 training
imprinting tests
1 h
18~36 h
30~60min
~24 h
red toy
linear
walking
vs
merged
Lp[red] and Wp[yellow]
imprinting_1 (biological)
Lp[red]
Wp[yellow]
imprinting_2 (artifact)
novel
familiar
B
BM score (sec)
walking
linear
(15)
(12)
(10)
(10)
control
VPA
ketamine
tubocurarine
C
a
imprinting_1 (biological) score (sec)
Wp[yellow]
Lp[red]
b
BM score (sec)
D
a
imprinting_2 (artifact) score (sec)
familiar (red)
novel (yellow)
b
control (15)
VPA (12)
ketamine (10)
tubocurarine (10)

figure_4

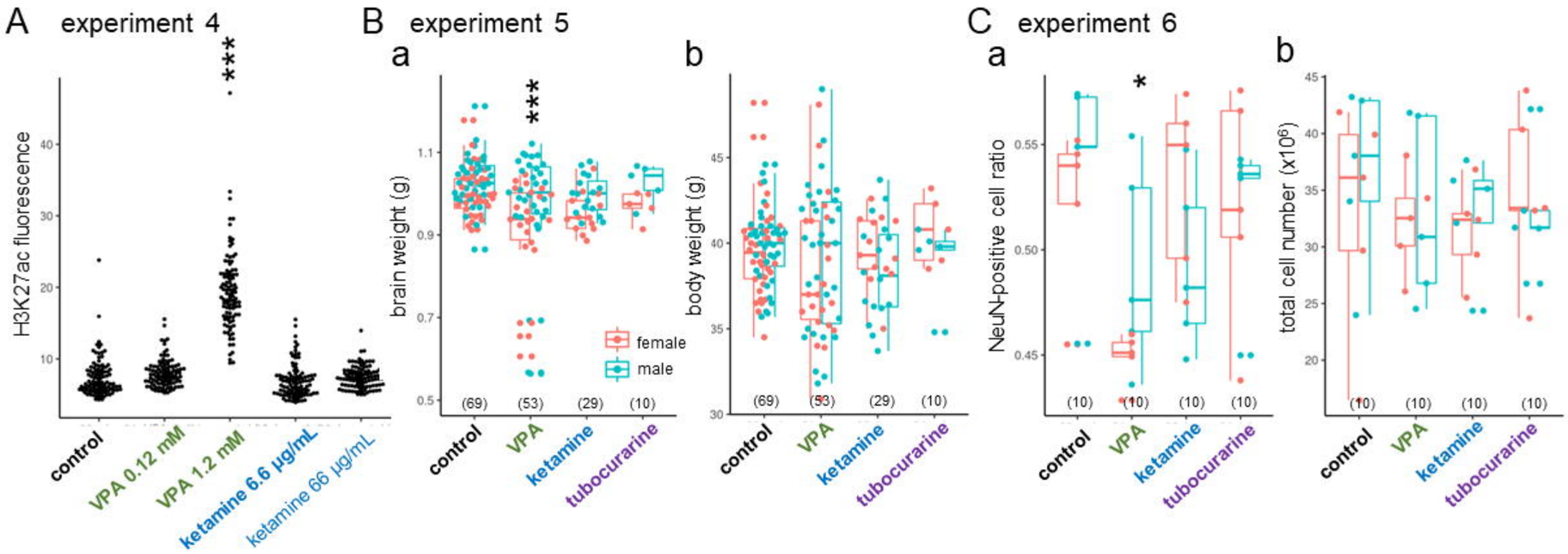
A experiment 4
H3K27ac fluorescence
control
VPA 0.12 mM
VPA 1.2 mM
ketamine 6.6 µg/mL
ketamine 66 µg/mL
B experiment 5
a
brain weight (g)
b
body weight (g)
female
male
(69) (53) (29) (10)
control
VPA
ketamine
tubocurarine
C experiment 6
a
NeuN-positive cell ratio
b
total cell number (x10^6)
(10) (10) (10) (10)

figure_5

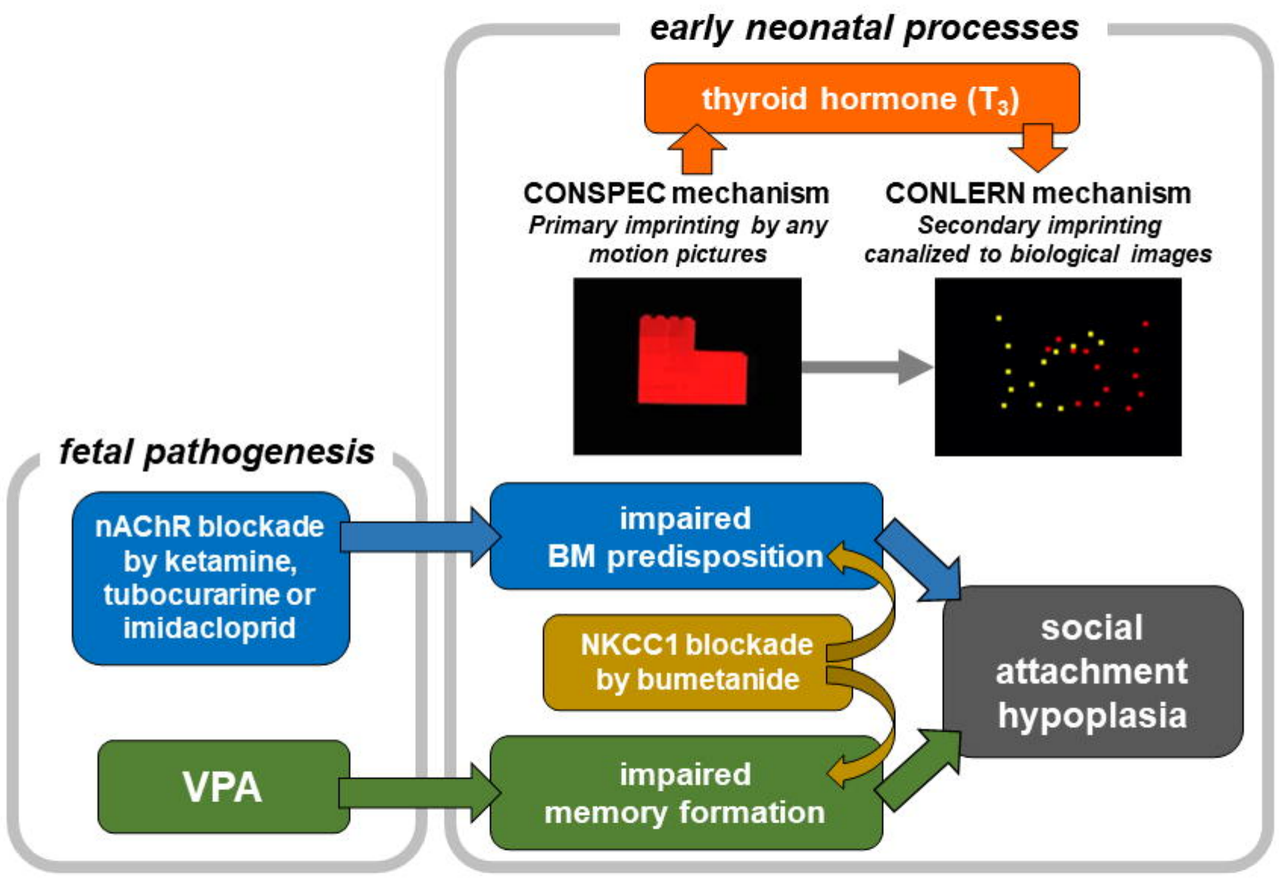
early neonatal processes
thyroid hormone (T_3)
CONSPEC mechanism
Primary imprinting by any motion pictures
CONLERN mechanism
Secondary imprinting canalized to biological images
fetal pathogenesis
nAChR blockade by ketamine, tubocurarine or imidacloprid
VPA
impaired BM predisposition
NKCC1 blockade by bumetanide
impaired memory formation
social attachment hypoplasia

figure_S1

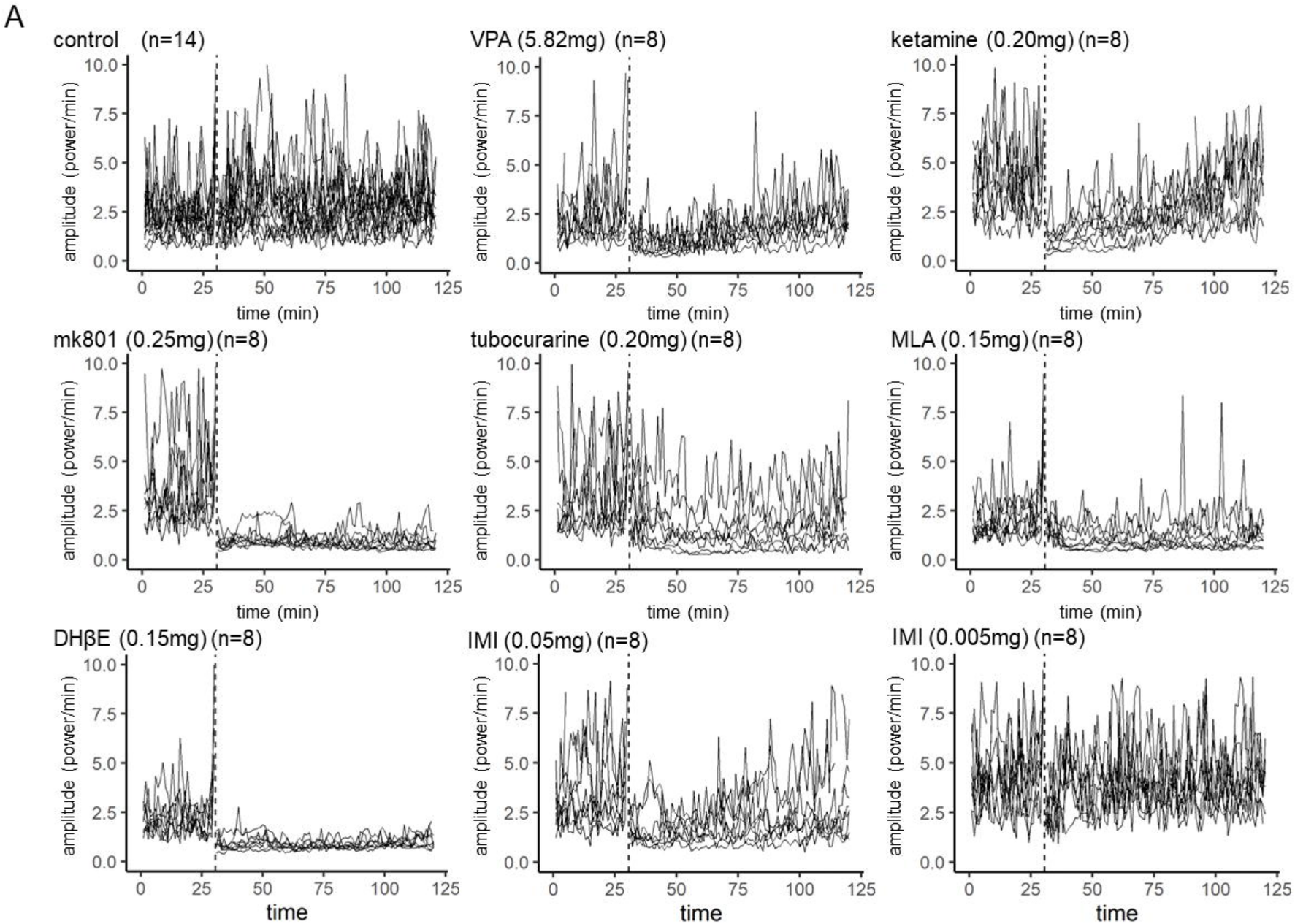
A
control (n=14)
VPA (5.82mg) (n=8)
ketamine (0.20mg) (n=8)
mk801 (0.25mg) (n=8)
tubocurarine (0.20mg) (n=8)
MLA (0.15mg) (n=8)
DHβE (0.15mg) (n=8)
IMI (0.05mg) (n=8)
IMI (0.005mg) (n=8)
amplitude (power/min)
time (min)
time
0.0
2.5
5.0
7.5
10.0
0
25
50
75
100
125

figure_S1

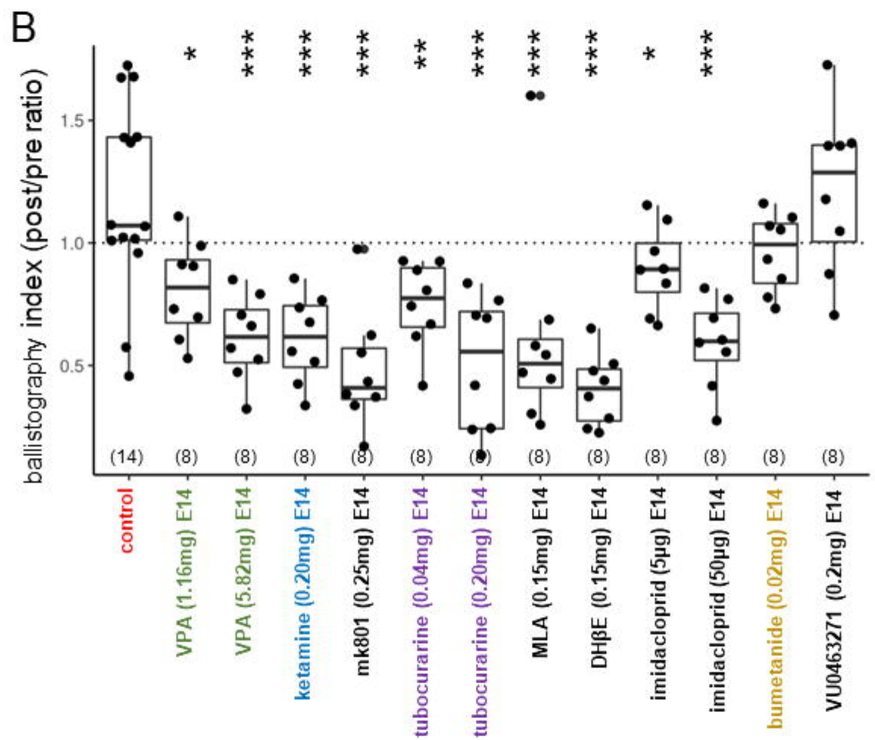
B
ballistography index (post/pre ratio)
1.5
1.0
0.5
*
***
***
***
**
***
***
***
*
***
(14)
(8)
control
VPA (1.16mg) E14
VPA (5.82mg) E14
ketamine (0.20mg) E14
mk801 (0.25mg) E14
tubocurarine (0.04mg) E14
tubocurarine (0.20mg) E14
MLA (0.15mg) E14
DHβE (0.15mg) E14
imidacloprid (5µg) E14
imidacloprid (50µg) E14
bumetanide (0.02mg) E14
VU0463271 (0.2mg) E14

figure_S2

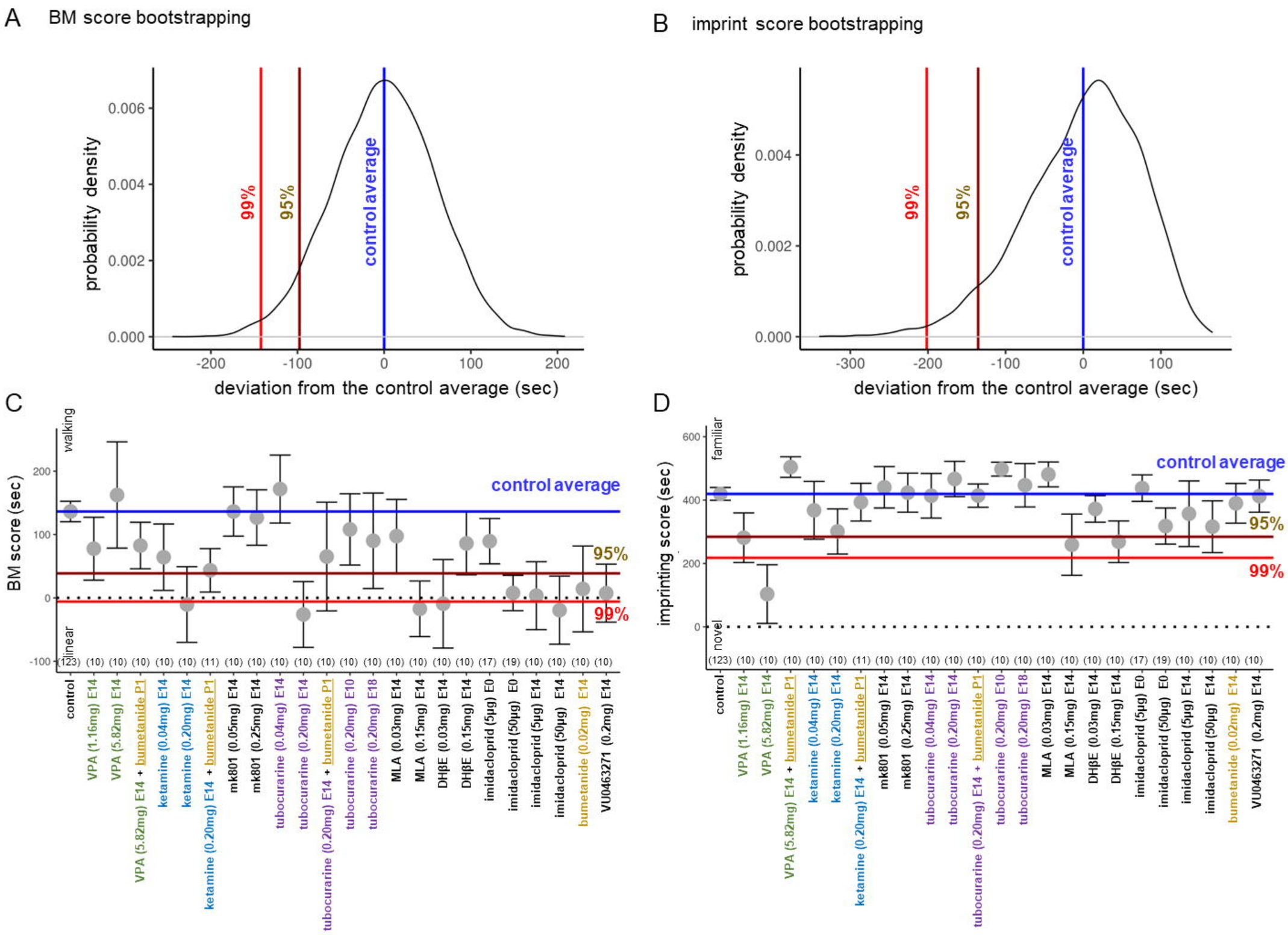
A
BM score bootstrapping
probability density
0.006
0.004
0.002
0.000
99%
95%
control average
-200
-100
0
100
200
deviation from the control average (sec)
B
imprint score bootstrapping
probability density
0.004
0.002
0.000
99%
95%
control average
-300
-200
-100
0
100
deviation from the control average (sec)
C
BM score (sec)
walking
linear
200
100
0
-100
control average
95%
99%
(123) (10) (10) (10) (10) (10) (11) (10) (10) (10) (10) (10) (10) (10) (10) (10) (10) (10) (17) (19) (10) (10) (10) (10)
control
VPA (1.16mg) E14
VPA (5.82mg) E14
VPA (5.82mg) E14 + bumetanide P1
ketamine (0.04mg) E14
ketamine (0.20mg) E14
ketamine (0.20mg) E14 + bumetanide P1
mk801 (0.05mg) E14
mk801 (0.25mg) E14
tubocurarine (0.04mg) E14
tubocurarine (0.20mg) E14
tubocurarine (0.20mg) E14 + bumetanide P1
tubocurarine (0.20mg) E10
tubocurarine (0.20mg) E18
MLA (0.03mg) E14
MLA (0.15mg) E14
DHβE (0.03mg) E14
DHβE (0.15mg) E14
imidacloprid (5μg) E0
imidacloprid (50μg) E0
imidacloprid (5μg) E14
imidacloprid (50μg) E14
bumetanide (0.02mg) E14
VU0463271 (0.2mg) E14
D
imprinting score (sec)
familiar
novel
600
400
200
0
control average
95%
99%
(123) (10) (10) (10) (10) (10) (11) (10) (10) (10) (10) (10) (10) (10) (10) (10) (10) (10) (17) (19) (10) (10) (10) (10)
control
VPA (1.16mg) E14
VPA (5.82mg) E14
VPA (5.82mg) E14 + bumetanide P1
ketamine (0.04mg) E14
ketamine (0.20mg) E14
ketamine (0.20mg) E14 + bumetanide P1
mk801 (0.05mg) E14
mk801 (0.25mg) E14
tubocurarine (0.04mg) E14
tubocurarine (0.20mg) E14
tubocurarine (0.20mg) E14 + bumetanide P1
tubocurarine (0.20mg) E10
tubocurarine (0.20mg) E18
MLA (0.03mg) E14
MLA (0.15mg) E14
DHβE (0.03mg) E14
DHβE (0.15mg) E14
imidacloprid (5μg) E0
imidacloprid (50μg) E0
imidacloprid (5μg) E14
imidacloprid (50μg) E14
bumetanide (0.02mg) E14
VU0463271 (0.2mg) E14